Identification and Characterization of Cancer Stem Cells Responsible for Drug-Resistance and Metastasis

January 2021

Shinta KOBAYASHI

Identification and Characterization of Cancer Stem Cells Responsible for Drug-Resistance and Metastasis

A Dissertation Submitted to

the Graduate School of Science and Technology,

University of Tsukuba

in Partial Fulfillment of Requirements

for the Degree of Doctor of Philosophy in Science

Doctoral Program in Biology,

Degree Programs in Life and Earth Sciences

Shinta KOBAYASHI

Table of Contents

General Abstract

Cancer stem cell (CSC) theory posits that a subset of cancer cells has the indefinite self-renewal ability to initiate and maintain tumor reconstitution. Therefore, tumors are organized in a hierarchical fashion, equivalent to the normal tissue hierarchy supported by stem cells. To accurately characterize CSCs, I focused on normal stem cell related molecules (LGR5: Leucine-rich repeat-containing G-protein-coupled Receptor 5 and Insm1: Insulinoma-associated protein 1) and evaluated the relationship between CSCs, drug resistance, and metastasis.

In colorectal tumors, LGR5-posotive ($LGR5^+$) cells were shown to have CSC properties. In the presence of anticancer drugs, $LGR5^+$ cells were transformed into LGR5-negative ($LGR5^-$) drug-resistant cells. Upon removal of anticancer drugs, $LGR5^-$ cells reverted to $LGR5^+$ and reconstituted hierarchical tumors *in vitro* and *in vivo*. In addition, I found that HLA-DMA and epiregulin (EREG) can be used as markers of $LGR5^-$ drug-resistant cells. Using these markers, I detected both $LGR5^+$ and HLA-DMA^+/$EREG^+$ cells in colon patients. For pancreatic neuroendocrine tumors, I used RIP1-Tag2 (RT2) transgenic mice to establish a functional tumor (RT2 B6) model and a non-functional stem cell type tumor (RT2 AB6F1) model. The results showed that

Insm1 was strongly expressed in RT2 B6, but only slightly expressed in highly metastatic RT2 AB6F1. Using human cell lines, *Insm1* deletion induced a CSC phenotype and increased cancer invasion *in vitro* and cancer metastasis rates *in vivo*. Thus, LGR5 and Insm1, which play important roles in normal stem cells, were found to be associated with drug resistance and metastasis in CSCs. The results provide new biological insights into drug resistance and metastasis of CSCs.

Abbreviations

ALDH	aldehyde dehydrogenase
AML	acute myelogenous leukemia
CBC	crypt base columnar
CHO	Chinese Hamster Ovary
CHTN	Cooperative Human Tissue Network
CMV	Cytomegalovirus
CSC	cancer stem cell
CSCs	cancer stem cells
DAPI	4',6-diamidino-2-phenylindole
DNA	deoxyribonucleic acid
DPBS	Dulbecco's Phosphate-Buffered Saline
EREG	Epiregulin
ELISA	Enzyme-Linked ImmunoSorbent Assay
EMT	Epithelial-Mesenchymal Transition
FBS	Fetal Bovine Serum
Insm1	Insulinoma-associated protein 1

LGR5	Leucine-rich repeat-containing G-protein-coupled Receptor 5
MRL/lprmice	MRL/MpJ-Tnfrsf6<lpr>/Crlj
NOG	NOD/Shi-scid, IL-2Rγnull
NF-PanNETs	nonfunctioning PanNETs
PanNETs	pancreatic neuroendocrine tumors
PCR	polymerase chain reaction
PE	R-phycoerythrin
Q-PCR	quantitative PCR
RNA	ribonucleic acid
RTPCR	reverse transcription polymerase chain reaction
RT2	RIP1-Tag2
shRNA	short hairpin RNA
siRNA	small interfering RNA
TIA	tumor initiating activity
TICs	tumor initiating cells

General Introduction

It is widely recognized that cancer is a heterogeneous disease, and it is increasingly considered that heterogeneity within tumors contributes to treatment failure, disease progression, recurrence, and metastasis (Hanahan & Weinberg, 2011). Tumor heterogeneity is formed by extracellular matrix, stromal cells, immune cells, and other cells, in addition to cancer cells. This complexity of the cancer may increase the adaptability of the tumor to external stimuli such as drugs and radiation therapy, ultimately contributing to treatment failure (Junttila and de Sauvage, 2013). Cancer cells themselves may also alter cancer characteristics such as proliferation, invasion, apoptosis, and metabolism. However, until recently, the mechanisms driving heterogeneity within tumors were not known.

Research on how cancer heterogeneity develops is being actively pursued. For example, advanced genome sequencing has demonstrated that cancers within patients are a heterogeneous mixture of genetically distinct subclones (Burrell et al., 2013, Greaves and Maley, 2012). In parallel, strong evidence is emerging that non-genetic determinants, primarily related to developmental pathways, contribute to functional heterogeneity (Dick, 2008, Mechaam and Morrison, 2013, Nguyen et al., 2012). These

non-genetic determinants are typically derived from normal stem cells that are capable of self-renewal, which results in the formation of CSCs. The CSCs form a hierarchically organized tumor with large populations of cell types, causing cancer heterogeneity. This CSC model has attracted considerable interest because CSCs appear to have clinically relevant properties.

The idea that cancer retains normal stem cell properties has a long history, and many studies suggest that differentiated cells are produced by stem cells in tumors (Cornheim, 1875, Pierce et al., 1960, Beilin et al., 1978, Bennett et al., 1978, Pierce and Cox, 1978, Hager et al., 1981, Pierce and Speers, 1988). Based on these studies, the CSC theory has been proposed. CSC research was accelerated by the development of flow cytometer technology in the 1990s; in acute myelogenous leukemia (AML), $CD34^+$ $CD38^-$ cells isolated by flow cytometers were shown to have a high tumor initiating activity (Lapidot et al., 1994). Furthermore, $CD34^+CD38^-$ cells were shown to form hierarchically organized tumors (Bonnet and Dick, 1997). These studies provided direct evidence in support of the CSC theory.

CSCs in solid tumors were first identified in human breast cancer (Al-Hajj et al., 2003). $CD44^+CD24^-$ cancer cells were capable of self-renewal, the tumors derived from these cells were histologically heterogeneous and similar to the parental tumor. These

results show that the CSC concept can be applied to solid tumors. Since the initial publication on breast cancer, the CSC principle has been applied to tumors of the brain (Singh et al., 2004), head and neck (Prince et al., 2007), pancreas (Hermann et al., 2007, Li et al., 2007), lung (Eramo et al., 2008), prostate (Collins et al., 2005, Patrawala et al., 2006), colon (O'Brien et al., 2007, Ricci-Vitiani et al., 2007), and sarcomas (Wu et al., 2007). In addition, CSC markers for each cancer type were identified.

A fundamental property of stem cells, whether normal or malignant, is self-renewal. Self-renewal is an important biological process in which stem cells produce asymmetric or symmetric daughter cells while retaining the ability to self-renew during cell division, and is important for maintaining stem cells. However, several studies have only addressed tumor-initiating activity, overlooking self-renewal capacity. As a result, cancer cells without self-renewal ability have also been reported as CSCs. To distinguish such cells, we call them tumor-initiating cells (TICs). CSCs and TICs have different characteristics, and a more accurate analysis of CSCs is needed to assess their intratumoral heterogeneity and their association with drug resistance, metastasis, and recurrence.

In this study, I analyze the relationship between CSCs, drug resistance and metastasis using a normal stem cell marker to accurately characterize CSCs. In Chapter

I, I identify colorectal CSCs using the normal intestinal stem cell marker, Leucine rich repeat containing G protein-coupled Receptor 5 (LGR5). LGR5 is expressed in the CBC (crypt base columnar) cells of the normal intestine, and $LGR5^+$ cells are known to be intestinal epithelial stem cells that differentiate into four types of cells (Barker et al., 2007). In addition, LGR5 activates the WNT signaling pathway by binding to the ligand R-spondin. The WNT signaling pathway plays a crucial role in embryonic development, tissue regeneration, and disease pathogenesis (Reya and Clevers, 2005) and is thought to be essential for stem cell self-renewal and maintenance (de Lau et al., 2011). By using specific antibodies against LGR5, $LGR5^+$ cells were purified and their CSC properties were evaluated. Purified $LGR5^+$ cells, not $LGR5^-$ cells, reconstituted the tumor hierarchy *in vivo*. With the medium containing R-spondin, $LGR5^+$ cells self-renewed under the adherent condition. In addition, $LGR5^+$ cells transitioned to $LGR5^-$ cells upon exposure to an anticancer drug, and these $LGR5^-$ cells reverted to $LGR5^+$ cells after culturing without an anticancer drug. Thus I find that $LGR5^+$ cancer cells maintain their stemness, convert to $LGR5^-$ drug-resistant cells, and reconstitute the tumor hierarchy.

In Chapter II, I analyze the function of Insulinoma-associated protein 1 (Insm1) in pancreatic endocrine tumors. Insm1 is a zinc finger transcription factor that is thought

to be essential for the development of pancreatic beta cells and enteroendocrine cells (Gierl et al., 2006). During pancreatic development, Insm1 promotes the transition from ductal progenitor cells to committed endocrine cells by regulating the expression of gene networks including *Neurog3* and *Ripply3* (Osipovich et al., 2014). Insm1 is also frequently expressed in insulinomas and other neuroendocrine tumors (Chen et al., 2019). Here I show that Insm1 was highly expressed in human insulinomas but unexpressed in NF-PanNETs. *Insm1*-deficient human cell lines expressed stem cell markers, were invasive *in vitro*, and metastasized at high rates *in vivo*. Thus I reveal that Insm1 can be used to identify whether a PanNET is a insulinoma or a metastatic stem cell type tumor, the deletion of *Insm1* induces a CSC phenotype and increases cancer metastasis.

By focusing on normal stem cell associated molecules (LGR5 and Insm1), I show that CSCs retain the properties of normal stem cells, and form cancer heterogeneity, leading to drug resistance and metastasis. The results of this study provide new biological insights into drug resistance and metastasis of CSCs.

Chapter1: LGR5-positive colon cancer stem cells interconvert with drug-resistant LGR5-negative cells

Abstract

The concept of CSCs has been proposed as an attractive theory for explaining the development of cancer, and the CSCs themselves have been seen as targets for the development of diagnosis and treatment. However, there remain many unanswered questions about drug-resistant CSCs. I report here the establishment of colon cancer CSC cell lines, the interconversion of CSCs between a rapid proliferating and a slow cycling state, and the reconstitution of the tumor hierarchy. Stable cell lines with CSC properties were established from human colon cancer following serial passages in NOD/Shi-scid, IL-2Rγnull (NOG) mice and subsequent adherent cell cultures. By generating specific antibodies against LGR5, I demonstrated that these cells express LGR5 and undergo self-renewal within the media containing R-spondin. To evaluate the drug sensitivity of these cells, $LGR5^+$ cells were treated with irinotecan, and resulted in their transformation into drug-resistant $LGR5^-$ cells. Furthermore, $LGR5^-$ cells converted to $LGR5^+$ after removal of irinotecan, then re-grew well. Analysis of DNA microarrays and immunohistochemistry revealed that HLA-DMA was specifically

expressed in drug-resistant $LGR5^-$ cells, and epiregulin was expressed in both $LGR5^+$ and $LGR5^-$ cells. In addition, these cells were found in the tumor tissue of colon cancer patients. These data demonstrate that $Lgr5^+$ cancer cells have stemness, convert to $LGR5^-$ drug-resistant cells, and reconstitute the tumor.

Introduction

In the normal intestine, LGR5 is initially identified as a marker of normal stem cells (Barker et al., 2007), and LGR5 activates the WNT signaling pathway by binding its ligand, R-spondin. The WNT signaling pathway plays a crucial role in tissue generation, and the WNT activation is thought to be essential for stem cell proliferation and maintenance (Reya and Clevers, 2005, de Lau et al., 2011). $LGR5^+$ normal stem cells self-renew upon activation of the WNT signaling. Similar to normal tissues, LGR5 is thought to play an important role in colorectal CSCs (Barker et al., 2009, Vermeulen et al., 2008, Takahashi et al., 2011, Takeda et al., 2011). For example, $LGR5^+$ cells formed adenomas by excessive activation of the WNT signaling, and LGR5 expression was observed in several colon cancer cell lines (Barker et al., 2009). Although it is clear that LGR5 is an important molecule for the identification of CSCs in the colon, it has not been evaluated as a CSC marker due to the lack of specific antibodies to LGR5, which is essential for the isolation and identification of CSCs.

The difficulties in studying CSCs are due to the heterogeneity of cell types and the rarity of CSCs in tumor tissues. There have been a lot of attempts to enrich and isolate CSCs with spheroid cultures *in vitro*, to sort cells with CSC markers, and to directly xenotransplant cancer cells in immunodeficient mice (Lapodpt., 1994, AI-Hajj

et al., 2003, Singh et al., 2004, O'Brien et al., 2007, Ricci-Vitiani et al., 2007). While these methods enrich CSCs, they produce heterogeneous cell populations and are not sufficiently effective at isolating and maintaining pure CSC populations (Vermeulen et al., 2010).

Here I report the identification and the establishment of human colon cancer cell lines that express LGR5 and possess CSC properties. Cell lines were created using serial passages of colorectal cancer cells xenotransplanted into NOG mice followed by an adherent cell culture. For this purpose, I generated antibodies that are specific to LGR5. Obtained $LGR5^+$ cells self-renewed under the culture condition with the medium containing R-spondin. In addition, $LGR5^+$ cells transitioned to $LGR5^-$ cells upon exposure to an anticancer drug, and these $LGR5^-$ cells reverted to $LGR5^+$ cells after culturing without an anticancer drug. Through gene expression profiling, I demonstrated that HLA-DMA, which belongs to the HLA class II alpha chain paralogues, is expressed in drug-resistant $LGR5^-$ cells and epiregulin (EREG), a member of the epidermal growth factor family, is expressed in both proliferating $LGR5^+$ and drug resistant $LGR5^-$ cells. By using antibodies against LGR5, HLA-DMA and EREG, I demonstrate the existence of $LGR5^+$ and $LGR5^-$ cells in tumor xenografts and in the tissues in colorectal cancer patients. This is the first stable cell line with CSC properties

and the ability to transition between a rapid proliferating and a slow cycling state. Thus, $LGR5^+$ colon CSCs interconvert with drug-resistant $LGR5^-$ cells and are capable of tumor reconstitution. This suggests the physiological importance of CSCs in tumor recurrence after drug treatment.

Materials and Methods

Preparation of monoclonal antibodies against LGR5

Anti-LGR5monoclonal antibodies, 2L36 and 2U2E-2, were obtained by DNA immunization and protein immunization, respectively. For DNA immunization, plasmid DNA encoding *LGR5* was transferred once a week 6 times to the abdominal skin of 6-week-old female MRL/lpr mice (MRL/MpJ-Tnfrsf6<lpr>/Crlj) (Charles River Japan) using a Helicos Gene Gun (BioRad) at a pressure of 200 to 300 psi. At the final immunization, $1x10^6$cells of CHO DG44 (Life technologies) expressing LGR5 were intravenously injected. The splenocytes were resected 3 days after the final immunization and fused with P3-X63-Ag8U1 mouse myeloma cells (ATCC). 2L36 was obtained by screening the culture supernatants of hybridoma by flow cytometry (Kremer et al., 2004).

The N-terminal region of LGR5 (amino acid 1-555) was expressed as a fusion protein with the Fc region of mouse IgG2a in CHO DG44 cells. The LGR5-Fc protein secreted in the culture medium was purified with HiTrap Protein A FF column (GE Healthcare), and then 6-week-old female Balb/c mice (Charles River Japan) were immunized subcutaneously with 50μg of the LGR5-Fc protein emulsified in Freund's Complete Adjuvant (Difco). Immunization was repeated once a week for two weeks

with the same amount of the LGR5-Fc protein in Freund's Incomplete Adjuvant (Difco). Three days before cell fusion, mice were injected intravenously with 25μg of the LGR5-Fc protein. Hybridomas were generated as described above, and the antibody 2U2E-2 was selected by ELISA with the LGR5-Fc protein.

Establishment of human colon cancer patient derived xenografts

Colon cancer specimens were obtained from consenting patients, as approved by the ethical committee at PharmaLogicals Research and Parkway Laboratory Services in Singapore. Pieces of tumors were minced with scissors and implanted into the flank of NOG mice (Central Institute for Experimental Animals). The human colon patient derived xenografts were maintained by passages in NOG mice. All studies and procedures involving animal subjects were approved by the Animal Care and Use Committee at PharmaLogicals Research and the Institutional Animal Care and Use Committee at Chugai Pharmaceutical Co., Ltd.

Establishment of colon cancer cell lines with cancer stem cell properties

Single cell suspension of cancer cells from the xenografts was prepared by mincing the tissues with scissors, incubated in DPBS containing collagenase/dispase (Roche) and DNase I (Roche) at 37°C for 3 hr followed by filtration with a 40 μm cell strainer (BD Biosciences) and suspending in red blood cells lysing buffer (BD

Biosciences). The cells were cultured in a stem cell medium [DMEM/F12 medium (Life technologies) supplemented with N-2 supplement (Life technologies), 20 ng/mL human EGF (Life technologies), 10 ng/mL human basic fibroblast growth factor (Sigma), 4 μg/mL heparin (Sigma), 4 mg/mL BSA (Life technologies), 20 μg/mL human insulin, zinc solution (Life technologies), and 2.9 mg/mL glucose (Sigma)] at 37°C under 5% CO_2 (Todaro et al., 2007). Drug resistant $LGR5^-$ cells were obtained by treating the adherent $LGR5^+$ cells with 10 μg/mL of irinotecan (Hospira) for 3 days.

Sorting of the $LGR5^+$ and $LGR5^-$ cells

The primary cells from xenografts were incubated with the anti-LGR5 antibody (2L36, 2 μg/mL) and then PE-labeled anti-mouse IgG2a (Life technologies, 1/200 dilution). Mouse cells were discriminated from the human colon cancer cells by staining with anti-mouse MHC class I antibody (Abcam, ERMP42, 0.1 μg/mL) and APC-labeled anti-rat IgG (BioLegend, 1/100 dilution). Dead cells were removed by 7-AAD Viability Dye (Beckman Coulter). Flow cytometry analysis and cell sorting were performed using a MoFlo XDP (Beckman Coulter) cell sorter.

Flow cytometry analysis

The cells were incubated with the labeled antibodies. Antibodies used were PE-labeled anti-CD133 antibody (Miltenyi Biotec, 1/11 dilution), PE-labeled anti-CD44

antibody (BD Bioscience, 1/11 dilution), FITC-labeled anti-EpCAM antibody (Miltenyi Biotec, 1/11 dilution), PE-labeled anti-CD166 antibody (R&D Systems, 1/25 dilution), PE-labeled anti-CD24 antibody (BD Bioscience, 1/11 dilution), PE-labeled anti-CD26 antibody (BD Bioscience, 1/11 dilution) and PE-labeled anti-CD29 antibody (BD Bioscience, 1/11 dilution). Activity of ALDH was analyzed using the AldeFluor Kit (StemCell Technologies) according to the manufacturer's instructions. Mouse cells were discriminated from the human colon cancer cells by staining with anti-mouse MHC class I antibody (Abcam, 0.1 μg/mL) and PE- or APC-labeled anti-rat IgG (BioLegend, 1/100 dilution). Dead cells were removed by 7-AAD Viability Dye (Beckman Coulter). Flow cytometry analysis was performed using an EPICS ALTRA (Beckman Coulter).

Tumor initiating activity (TIA) assay

Cells suspended in Hank's balanced salt solution (Life technologies) with 50% matrigel were subcutaneously inoculated into the flanks of NOG mice. For single cell inoculation, cells were stained with FITC-labeled anti-EpCAM antibody (MiltenyiBiotec, 130-080-301) and seeded in Terasaki plates (Thermo Fisher Scientific). Single-cell observation can be accurately performed on the Terasaki plate. After the presence of a single cell in each well was confirmed under a fluorescence

microscope, the single cell in 50μL of 50% matrigel was inoculated into the flank of mice.

Histological examination

Small pieces of surgical specimens of human tissues and of the xenograft tumor tissues were fixed with 4% paraformaldehyde at 4°C for 16 to 24 hr and embedded in paraffin by the AMeX method (Sato et al., 1986, Suzuki et al., 2002). After washing the *in vitro* cultured cells with PBS-EDTA, the cells were fixed with 4% paraformaldehyde at 4°C for 2 hr, suspended in 0.5 mL agarose, and embedded in paraffin with the AMeX method. Thin sections were subjected to hematoxylin & eosin staining and to immunohistochemistry.

Immunohistochemistry

Thin sections from the above mentioned paraffin blocks were incubated with anti-LGR5 antibody (2U2E-2, 1μg/mL), anti-EREG antibody (10μg/mL), anti-E-cadherin antibody (Abcam, 2.5μg/mL), anti-HLA-DMA antibody (Sigma, 2.5μg/mL) or FITC-labeled anti-Ki67 antibody (Abcam, 2.5 μg/mL). After the incubation with the primary antibodies, the sections were incubated with a secondary antibody conjugated with polymer-HRP (DAKO or Vector Laboratories) or biotin, and the proteins were visualized by AlexaFluor 488-labeled tyramide (Life technologies, 1/100 dilution),

AlexaFluor 568-labeled tyramide (Life technologies, 1/100 dilution), or AlexaFluor 568-labeled streptavidin (Life technologies, 2μg/mL). For immunofluorescent cytochemistry, cells were fixed with 4% paraformaldehyde and permeabilized with 0.1% Triton-X 100 (Sigma), and incubated with anti-LGR5 antibody (2L36, 2 μg/mL). After the incubation with the primary antibodies, the cells were incubated with AlexaFluor 488-labeled anti-mouse IgG (Life technologies, 1/100 dilution). Those specimens and cells were also stained with DAPI (Life technologies).

Induction of the transition between LGR5$^+$ and LGR5$^-$ states in single cell culture

LGR5$^+$ cells were sorted with an anti-LGR5 antibody, and single LGR5$^+$ cells were cultured in 96-well microplates. To obtain drug resistant LGR5$^-$ cells, LGR5$^+$ cells were treated with 10 μg/mL of irinotecan for 3 days. Single LGR5$^-$ cells were cultured in 96-well microplates for 4 days. The medium used for the single cell culture contained 10% conditioned medium of the *in vitro* cultured LGR5$^+$ cells under an adherent condition. LGR5$^+$ and LGR5$^-$ states of the cells were confirmed by immunocytochemical analysis with anti-LGR5 antibody.

Statistical analysis

The Mann-Whitney *U* test was applied to determine the statistical significance of the differences in the numbers of tumor nodules in a metastatic tumor model. The

statistical analysis was carried out with an SAS preclinical package (SAS Institute, Inc.). *P* values smaller than 0.05 were considered significant.

Results

Generation and characterization of specific antibodies against LGR5

An antibody specific to LGR5 is essential for the isolation and characterization of CSCs in the colon, but such antibody has not been yet available. Therefore, I aimed to generate anti-LGR5 antibodies which allow me to isolate and analyze cells with CSC properties of the colon. Two monoclonal antibodies, 2L36 and 2U2E-2, specific to LGR5 were obtained. The regions of the LGR5 protein that contain epitopes of these antibodies are shown in Fig. 1A. Both antibodies were tested by immunohistochemistry and flow cytometry using the CHO cells expressing LGR5 or highly related proteins LGR4, or LGR6.When used for immunostaining, both 2L36 and 2U2E-2 recognized CHO cells expressing LGR5 but not those expressing LGR4 or LGR6 (Fig. 1B). In flow cytometry analysis, only 2L36 had a strong reaction with CHO cells expressing LGR5 (Fig. 1C). Furthermore, the 2U2E-2 antibody reacted specifically with crypt base columnar cells in the normal human intestine (Fig. 1D).

Human colon patient derived xenografts with cancer stem cell properties

Previously, 11 human colon patient derived xenografts using NOG mice were established (Fujii et al., 2008). I used two moderately differentiated colon cancer xenografs, PLR59 and PLR123. These xenografts were chosen because they grew more

rapidly while maintaining the ability to reconstitute tumors with epithelial ducts and small budding clusters even after ten passes in NOG mice (Fig. 2A). In the epithelial ducts of the tumors, differentiated cancer cells that showed a goblet cell-like phenotype were also observed in the xenotransplanted tumor tissues (Fig.2A inset). To confirm the presence of CSCs in xenotransplanted tumor tissues, I used immunohistochemical staining for the LGR5 protein that marks the CSCs of the colon. A small number of $LGR5^+$ cells were detected in the original tumor tissues and the passaged xenografts of PLR59 and PLR123 (Fig.2B).

Tumorigenicity of the sorted $LGR5^+$ and $LGR5^-$ cells

In order to examine the ability of $LGR5^+$ and $LGR5^-$ cells to form tumors *in vivo*, I sorted the $LGR5^+$ and $LGR5^-$ populations from the primary cells of patient-derived xenografts. Anti-LGR5 antibody 2L36 was used for the cell sorting. About 93% of the cells in the $LGR5^+$ fraction were $LGR5^+$, and more than 99% of the cells in the $LGR5^-$ fraction were $LGR5^-$ (Fig. 3A). When 1,000 cells were subcutaneously injected into NOG mice, the sorted $LGR5^+$ cells formed large visible tumors by day 34 after the inoculation, but the $LGR5^-$ cells gave rise to only very tiny tumors by day 34 (Fig. 3B).

Cancer stem cell properties of the established colon cancer cell lines

The main properties of CSCs are self-renewal, TIA and the reconstitution of a tumor tissue hierarchy of differentiated cells. In an attempt to establish cell lines with CSC properties, I used adhering cultures of cells derived from PLR59 and PLR123 xenografts in which the existence of $LGR5^+$ cells was confirmed (Fig. 4A). When the cells derived from PLR59 and PLR123 were cultured in an adherent condition with the medium containing R-spondin, the cells grew fast with a doubling time of approximately 2.5 days and showed epithelial morphology (Figs.4B, 4E).

In the TIA assay using NOG mice, the subcutaneous injection of 10 cells from primary tumors did not reconstitute the tumors, while 10 cells from adhering cultures formed tumors in all six injection sites, and even one single cell injection of an adhering cell reconstituted the tumors. The adherent culture has been effectively enriched with TIA-bearing cells. The histological morphology of the tumors from the adherent cells was almost identical to that of the original tumors (Fig.4C). Moreover, the TIA of the adhering cells was maintained even after the cells were cultured for more than a month.

Surface markers for PLR59 and PLR123 adherent cells were examined and found to be clearly positive for all previously reported known colon CSC markers: $LGR5^+$, $ALDH^+$, $CD133^+$, $CD44^+$, $EpCAM^+$, $CD166^+$, $CD24^+$, $CD26^+$ and $CD29^+$ (Fig.4D). Additionally, expression of the cell surface markers remained unchanged even

after one month of cell culture. One of the characteristics of CSCs is the symmetric cell division for self-renewal. The $LGR5^+$ adherent cells divided symmetrically in the adherent culture conditions with the medium containing R-spondin (Fig.4E). R-spondin induced self-renewal of CSCs. In the presence of matrigel and FBS, however, $LGR5^+$ cells underwent asymmetric cell divisions, as demonstrated by the segregation of LGR5 protein into one of two daughter cells (Fig.4F), generating two different daughter cells.

Interconversion between $LGR5^+$ proliferating and $LGR5^-$ drug-resistant states

I next asked whether the $LGR5^+$ cells exhibited a drug-resistant state, which is considered to be a typical feature of CSCs. I treated CSC cell lines (PLR59 and PLR123) and commercially available colon cancer cell lines (HCT116, HT-29 and LOVO) with irinotecan for 3 days. In CSC cell lines, about 80% of the cells were resistant to irinotecan. In addition, CSC cell lines regrew well after removal of irinotecan. On the other hand, only 30% of HCT116 cells were resistant to irinotecan and no regrowth was observed. None of the HT-29 and LOVO cells survived with irinotecan treatment (Figs. 5A, 5B).

Following treatment of the CSCs with irinotecan for 3 days, the surviving cells became $LGR5^-$, although they retained other colon CSC markers (Figs. 6A, 6B). After removal of irinotecan, $LGR5^-$ drug-resistant cells became positive for LGR5 and

resumed proliferation after re-culture (Figs.6A, 6B). In order to exclude the possibility of cell contamination, the transition from the $LGR5^+$ state to an $LGR5^-$ state and vice versa was also confirmed by observation of single cells in culture. When single $LGR5^+$ cells were cultured in multiwell plates, the cells transitioned to an $LGR5^-$ state within 3 days after irinotecan treatment. When single $LGR5^-$ cells treated with irinotecan were cultured in multiwell plates without irinotecan, 19 to 43% of the cells converted to the $LGR5^+$ state within 4 days (Fig. 6C). It was confirmed that the contaminated $LGR5^+$ cells did not survive. In order to confirm the proliferation of the $LGR5^+$ cells and drug-resistant $LGR5^-$ cells, I also double stained LGR5 and Ki67 with the *in vitro* cultures of the $LGR5^+$ and the $LGR5^-$ cells. The expression of LGR5 correlated well with Ki67 staining: $LGR5^+$ cells were positive for Ki67, and $LGR5^-$ drug-resistant cells were negative for Ki67 (Fig. 6D).

Identification of specific marker for $LGR5^-$ cells

To detect drug-resistant $LGR5^-$ cells, I attempted to identify the genes that are upregulated in the drug-resistant $LGR5^-$ cells by comparing the gene expression profiles of the drug-resistant $LGR5^-$ cells, the $LGR5^+$ cells, and the primary cells from the xenografts. From gene expression analyses of DNA microarray, the first 20 genes encoding membrane proteins with the biggest change are shown in heatmap (Fig. 7A).

Genes that have increased mRNA expression in drug-resistant LGR5$^-$ cells include MHC class II related genes (*HLA-DMA, HLA-DMB*), adhesion molecule related genes (*AMIGO2, FLRT3, GJB5, CLDN1*), G-protein coupled receptor protein signaling pathway related genes (*GPR87, GPR110, GPR172B, GNAI1, ABCA1*) and immune signaling related genes (*TNFSF15, BLNK, FAS, TMEM173*).

Immunohistochemical staining of cells cultured *in vitro* with antibodies confirmed that HLA-DMA was quite specifically expressed in the drug-resistant LGR5$^-$ cells (Fig. 7B). HLA-DMA was located in intracellular vesicles, and therefore could not be used for cell sorting. Nevertheless, HLA-DMA can be a useful molecule for the identification of the LGR5$^-$ cells in xenografts as well as in clinical specimens. I also looked for genes that were expressed in both LGR5$^+$ and drug-resistant LGR5$^-$ cells and identified EREG (Fig.7A). Immunohistochemical staining with a monoclonal antibody to EREG confirmed the expression of EREG in LGR5$^+$ and LGR5$^-$ cells (Fig.7B). By combining these markers, LGR5$^-$ cells can be detected as HLA-DMA and EREG double positive cells.

Reconstitution of the epithelial cell type tumor hierarchy from LGR5$^+$ cells

I next examined the possibility of converting LGR5$^+$ cells into drug-resistant cells *in vivo*. NOG mice with LGR5$^+$ cell-derived tumors were administered

intraperitoneally with 120 mg/kg of irinotecan. Tumor growth was almost completely inhibited (Fig.8A) and ductal structures were mostly destroyed (Fig.8B). In these conditions, the $LGR5^+$ cells were markedly decreased (Fig.8B). There was a significant increase in HLA-DMA-positive cells, which are $LGR5^-$, after irinotecan treatment. In contrast, about one-third of the cancer cells were $LGR5^+$ in the vehicle-treated control mice. Both $LGR5^+$ cells and HLA-DMA^+/$LGR5^-$ cells were positive for EREG (Fig.8B). The $LGR5^+$ cells reappeared after stopping irinotecan treatment (Fig.8B). As a result, tumor reconstitution occurred through the $LGR5^+$ cells.

The existence of both $LGR5^+$ and $LGR5^-$ cells in human colon cancers

I questioned whether $LGR5^+$ and $LGR5^-$ cells could be detected in tissue samples of clinical colon cancers. While rare, the $LGR5^+$ cells and the $LGR5^-$ cells that were HLA-DMA^+/$EREG^+$ were present in patients' primary colon cancer tissues (Fig.9A). Of the 12 cancer tissues in the human colon, both $LGR5^+$ and $LGR5^-$ cells were detected in 8 cases, and either $LGR5^+$ or $LGR5^-$ cells were found in the other 4 cases. The percentages of the $LGR5^+$ and $LGR5^-$ cells in those cases ranged between 0.003-1.864% for the $LGR5^+$ and 0.001-0.243% for the $LGR5^-$ cells. Both $LGR5^+$ and $LGR5^-$ cells were detected in ducts and budding areas (Fig.9A). Furthermore, in clinical

specimens, $LGR5^+$ cells were positive for Ki67, and $LGR5^-$/HLA-DMA^+ cells were negative for Ki67 (Fig. 9B).

DISCUSSION

Stem cell markers such as CD133, CD44, CD166, and ALDH have been used to identify and isolate colon CSCs (O'Brien et al., 2007, Ricci-Vitiani et al., 2007). Colon CSCs have been found in cell subpopulations positive for these markers; however, none is a definitive marker for colon CSCs. There is evidence that LGR5 marks normal intestine stem cells (Barker et al., 2007, Barker et al., 2009). In spite of this evidence, LGR5 remains unexplored in human CSCs due to a lack of specific antibodies (Barker et al., 2010). In this study, I have successfully generated monoclonal antibodies that are highly specific to LGR5 that can be applied to immunostaining, flow cytometry, and cell isolation. With the help of these unique LGR5 antibodies, I was able to define $LGR5^+$ cells as proliferating colon CSCs. In the development of pure CSC cell lines, I examined whether spheroid or adherent cultures would be useful for the enrichment of CSCs. Many attempts have been made to isolate and enrich CSCs *in vitro* using spheroid cultures (Vermeulen et al., 2008, Vermeulen et al., 2010). Findings from this study showed that in spheroid cultures $LGR5^+$ cells self-renewed and differentiated *in vitro*, resulting in a heterogeneous cell population as reported in other studies (Vermeulen al., 2008, Emmink et al., 2010). By contrast, adherent cultures with the medium containing R-spondin maintained only self-renewed $LGR5^+$ cells and prevented

their differentiation. Thus, adherent $LGR5^+$ cell lines are a highly homogeneous cell population with CSC characteristics and strong TIA. Only a few reports on the utilization of adherent culture for CSCs have been published on gliomas and breast cancer (Pollard et al., 2009, Scheel et al., 2011). In this study, I found a new potential for adherent cultures in isolating stable cell lines with CSC characteristics.

Based on established $LGR5^+$ cell lines, definitive evidence was obtained for $LGR5^-$ subpopulations resistant to anticancer drugs such as irinotecan. $LGR5^+$ cells exhibited a number of CSC features such as symmetric and asymmetric cell division, TIA, and the ability to produce a tumor hierarchy of different cell types. Furthermore, these cell lines interconverted between two separate states, a $LGR5^+$ proliferation state and a $LGR5^-$ slow cycling drug resistance state. While the formation of tumors from drug-resistant $LGR5^-$ cells in NOG mice was observed, the TIA of drug-resistant $LGR5^-$ cells was slightly lower than that of $LGR5^+$. Drug-resistant $LGR5^-$ cells were initially converted into $LGR5^+$ cells when tumor hierarchy was established *in vivo*. *In vivo* irinotecan treatment results suggest that anticancer drugs induce the transition of $LGR5^+$ cells into $LGR5^-$ drug-resistant cells, and these drug-resistant cells revert into $LGR5^+$ cells after the drug treatment has been discontinued. I was able to detect $LGR5^+$ and $LGR5^-$ cells in the tissues of colorectal cancer patients. These findings may explain why

some rare populations of CSCs survive drug therapy and result in tumor recurrence. If this hypothesis is correct, the CSC cell line provides a new way to test drugs that kill all the cancer cells in a tumor.

CSCs self-renew and produce differentiated cancer cells. In fact, $LGR5^+$ cells exhibited the ability to undergo asymmetric cell division, generating two different daughter cells *in vitro* and reconstituting tumor hierarchy *in vivo*. However, it is still unknown whether there is a transition from differentiated cancer cells to CSCs. Gupta et al. proposed a stochastic state transition of cancer cells (Gupta et al., 2011). Using breast cancer cell lines, they demonstrated that differentiated cancer cells possessed plasticity and changed to CSCs to maintain phenotypic proportions within tumors, although the frequency was very low (between 0.01% and 0.1%). In this study, tumor formation was detected in the 99.2% pure $LGR5^-$ population, which is considered to be differentiated tumor cells. Therefore, the potential for differential cell reversion to CSCs cannot be excluded.

I have established human colon cancer cell lines that express LGR5 and possess CSC properties. After treatment of the proliferating $LGR5^+$ cells with an anticancer agent, the $LGR5^+$ cells changed to a drug-resistant $LGR5^-$ state. In addition, the $LGR5^-$ cells converted to an $LGR5^+$ state in the absence of the drug, suggesting the presence of

CSCs capable of interconverting between the two different states to adapt to the external environment. Using antibodies against LGR5, HLA-DMA, and EREG, I show the existence of $LGR5^{+}$ and $LGR5^{-}$ cells in xenotransplanted tumor tissues and in human colon cancer tissues from patients. This suggests the clinical importance of CSCs in drug resistance and tumor recurrence.

Figures

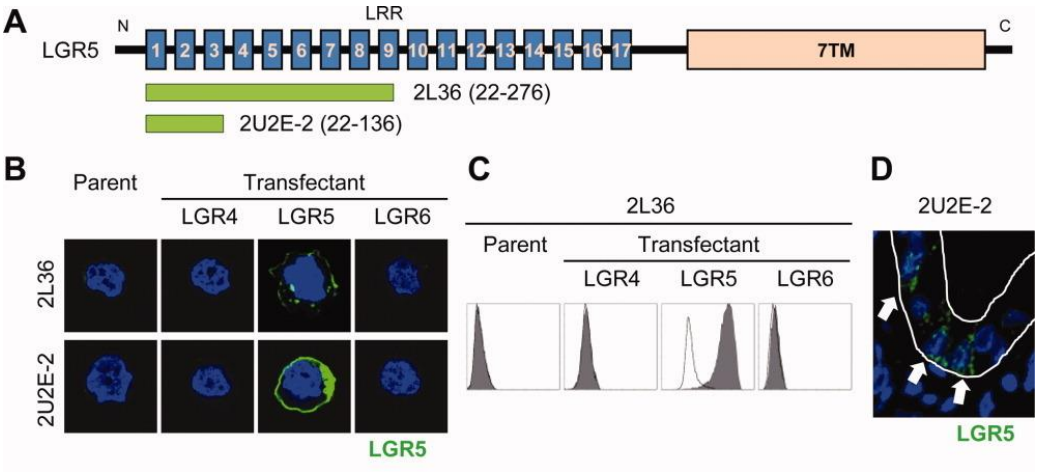

Figure. 1: Antigen-specific binding of anti-LGR5 antibodies.

(A): Regions of the LGR5 protein that contain epitopes of the anti-human LGR5 monoclonal antibodies, 2L36 and 2U2E-2. The monoclonal antibodies, 2L36 and 2U2E-2, were obtained by immunizing the LGR5 cDNA and N-terminal region of the protein, respectively. Green bars correspond to the regions containing epitopes. **(B, C)**: Specific binding of the anti-LGR5 antibodies to the antigen. **(B)**: Immunocytochemistry of CHO DG44 cells transfected with the LGR4, LGR5, or LGR6 cDNA. 2L36 and 2U2E-2 recognized the cells expressing LGR5 but not those expressing LGR4 or LGR6. **(C)**: Flow cytometry analysis of CHO DG44 cells transfected with the LGR4, LGR5, or LGR6 cDNA. 2L36 reacted with the cells expressing LGR5 but not those expressing LGR4 or LGR6. **(D)**: Staining of the crypt base cells in normal human intestine. The

thin sections of the normal human intestine were stained with 2U2E-2. Specific fluorescence was observed in the crypt base columnar cells (arrows).

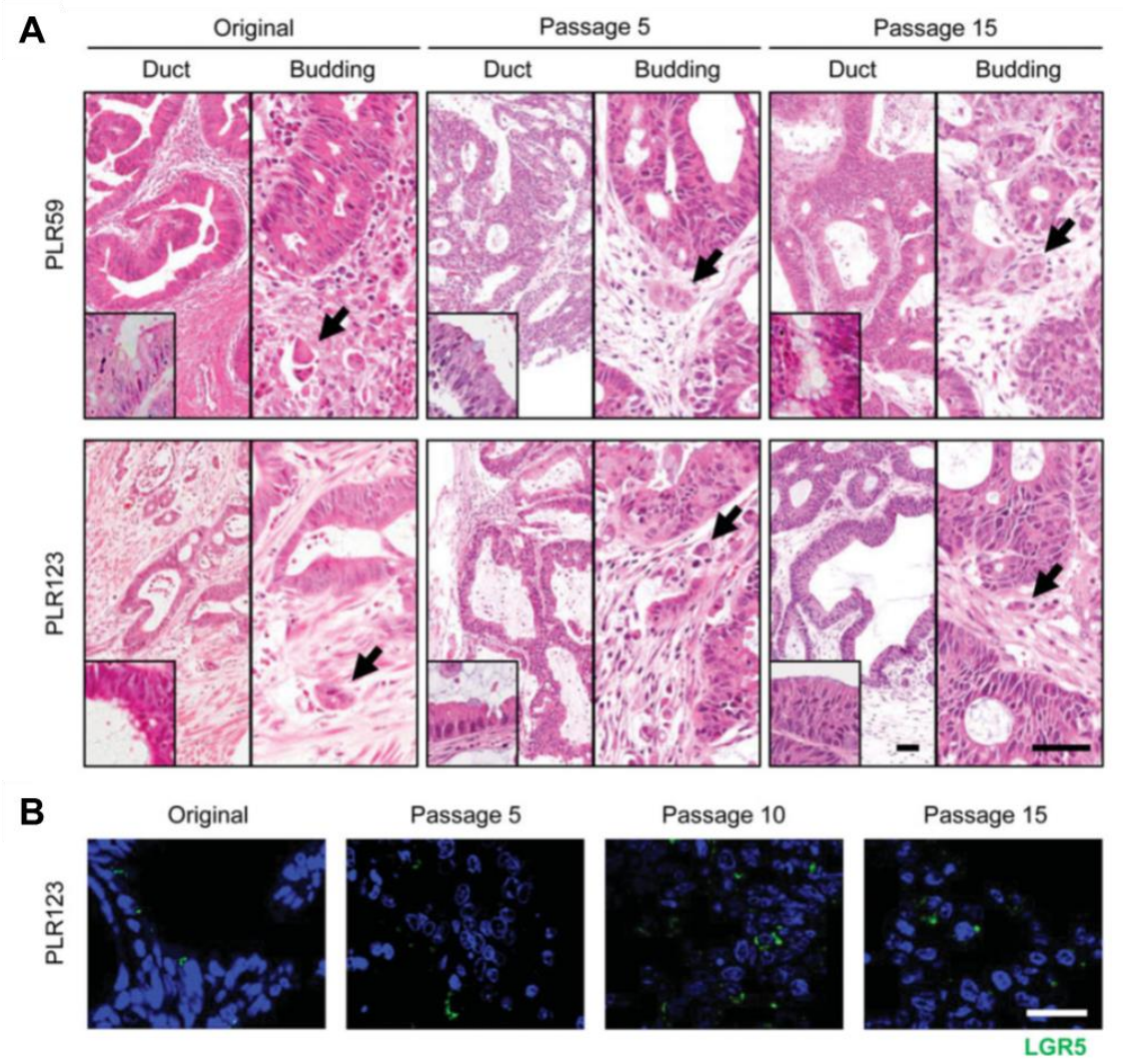

Figure. 2: Characteristics of human colon patient derived xenografts, PLR59 and PLR123

(A): Histology of surgically resected tumors of PLR59 and PLR123 and xenograft tumor tissues. Tumors derived from PLR59 and PLR123 had tubular structures containing goblet cells (inserts) and budding cluster (arrows). Bar = 50 μm. (B): Immunostaining of LGR5 in the surgically resected tumors (PLR123) and xenografts

derived from PLR123. Sections were stained with the anti-LGR5 antibody. Bar = 25 μm. Original, surgically resected tumors from patients.

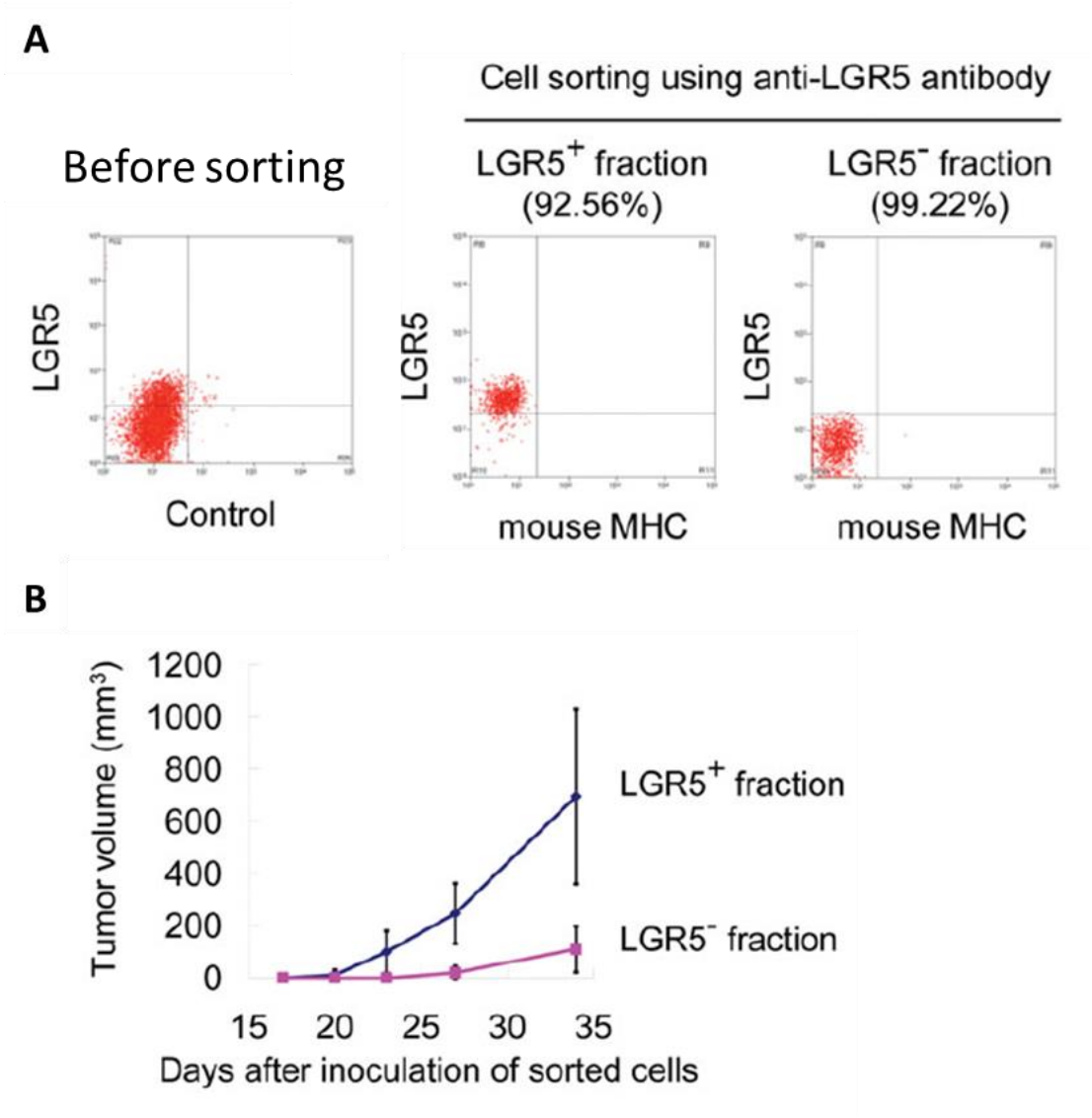

Figure 3. Tumorigenicity of the sorted LGR5$^+$ and the LGR5$^-$ cells.

(A): Flow cytometry analysis of the sorted LGR5$^+$ and LGR5$^-$ populations from the primary cells of PLR123 xenografts. Percentages indicate the purity of the sorted cell population. **(B)**: Tumor formation by the sorted LGR5$^+$ and the LGR5$^-$ cells. One thousand cells of the sorted LGR5$^+$ and the LGR5$^-$ populations suspended in Matrigel

were subcutaneously inoculated into NOG mice, and tumor volume was measured.

Mean ± SD of six tumors is shown.

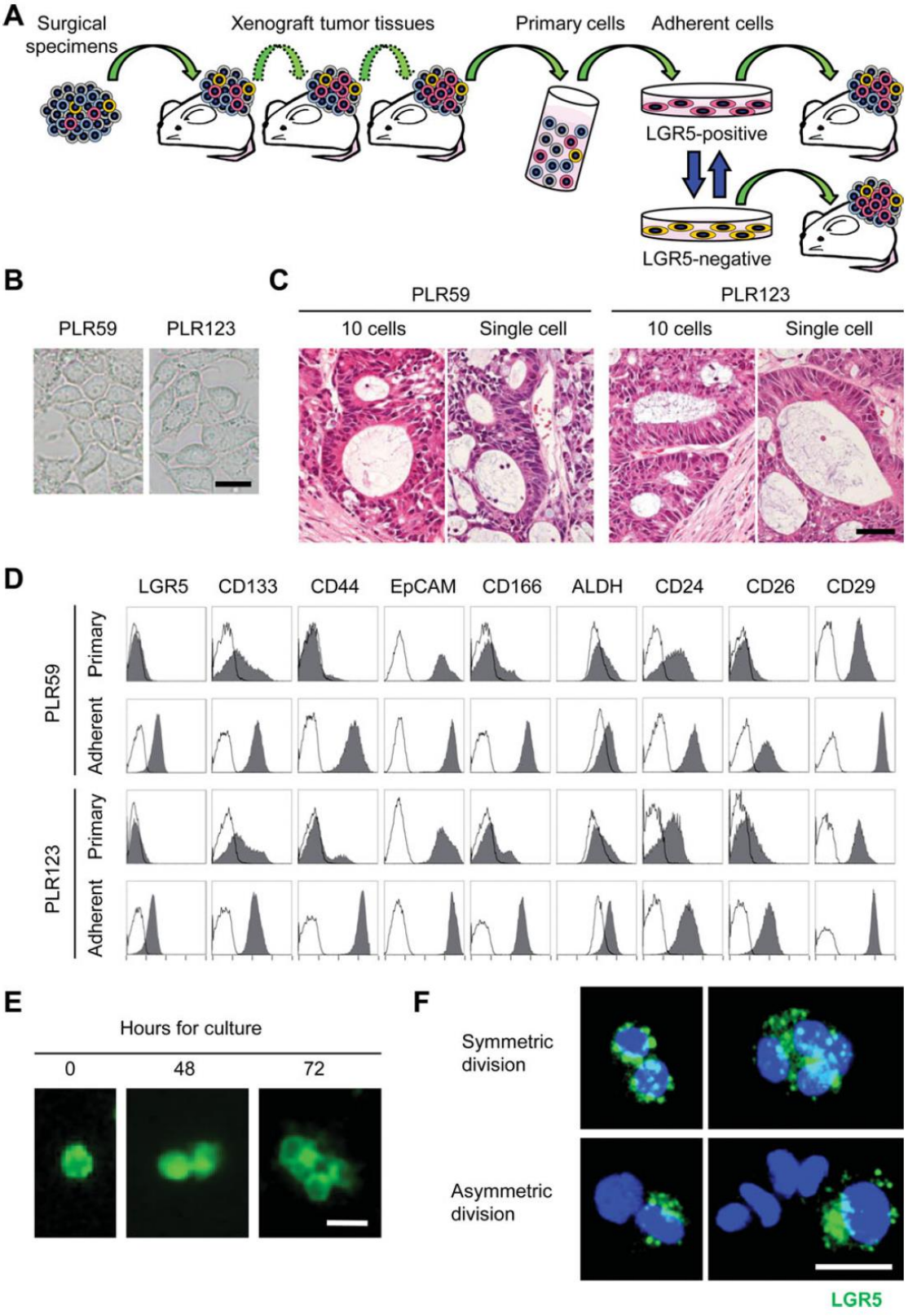
A
Surgical specimens
Xenograft tumor tissues
Primary cells
Adherent cells
LGR5-positive
LGR5-negative
B
PLR59
PLR123
C
PLR59
PLR123
10 cells
Single cell
10 cells
Single cell
D
LGR5
CD133
CD44
EpCAM
CD166
ALDH
CD24
CD26
CD29
PLR59
Primary
Adherent
PLR123
Primary
Adherent
E
Hours for culture
0
48
72
F
Symmetric division
Asymmetric division
LGR5

Figure 4. Characteristics of colon cancer cell lines with cancer stem cell properties.

(A): Schematic representation of the process of establishing colon cancer cell lines. **(B)**: Phase contrast microscopy of the cells in the $LGR5^+$ cell lines. Cells were collected from xenografts of PLR59 and PLR123 after more than 10 passages in NOD/Shi-scid, IL-2R γ null (NOG) mice and cultured under an adherent culture condition. Bar = 20 μm. **(C)**: Histology of the tumors derived from the $LGR5^+$ cells from PLR59 and PLR123 xenografts. Ten or single $LGR5^+$ cells from the adherent cultures of the cells derived from PLR59 and PLR123 xenografts were subcutaneously injected into NOG mice. Bar = 50 μm. **(D)**: Expression of CSC markers. The primary cells from xenografts of PLR59 and PLR123 after more than 10 passages in NOG mice (upper) and the $LGR5^+$ cells cultured under an adherent culture condition (lower) were analyzed by flow cytometry. Shadow, Fluorescent intensities after staining with the indicated antibodies or ALDH activity; Open, Fluorescent intensities after staining with control isotype antibody or ALDH activity with an ALDH inhibitor. **(E)**: Symmetric division of the $LGR5^+$ cells. The $LGR5^+$ cells stained with PKH67 dye were cultured for 72 hours and examined by fluorescent microscopy. Bar = 20 μm. **(F)**: Symmetrical (upper) and asymmetrical (lower) divisions of the $LGR5^+$ cells in the presence or absence of Matrigel and fetal bovine serum. Photographs of the cells were taken after single

division (left) and after two or three divisions (right). The $LGR5^+$ cells were cultured for 48‑72 hours and stained with the anti-LGR5 antibody. Bar = 20 μm.

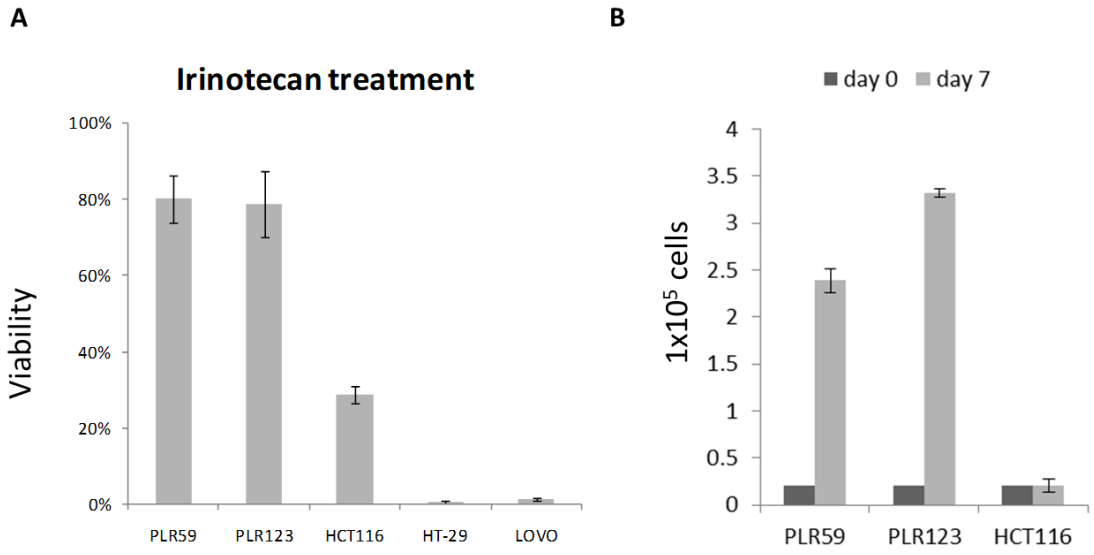

Figure 5. Effect of irinotecan on survival and re-growth of LGR5$^+$ cells.

(A): Percentage of viable cells after treatment of irinotecan. After treatment of the CSC cell lines (PLR59 and PLR123), HCT116, HT-29 and LOVO cells with 10 μg/mL irinotecan for 3 days, percentage of viable cells was calculated. The results are the mean of three independent experiments. Bars on each column indicate standard deviations.

(B): Growth of drug resistant cells from PLR59, PLR123, and HCT116. $3x10^4$ cells were cultured for 7 days under an adherent condition, and number of viable cells were counted. Black column: number of viable cells when seeded, Gray column: number of viable cells after culturing the cells for 7 days.

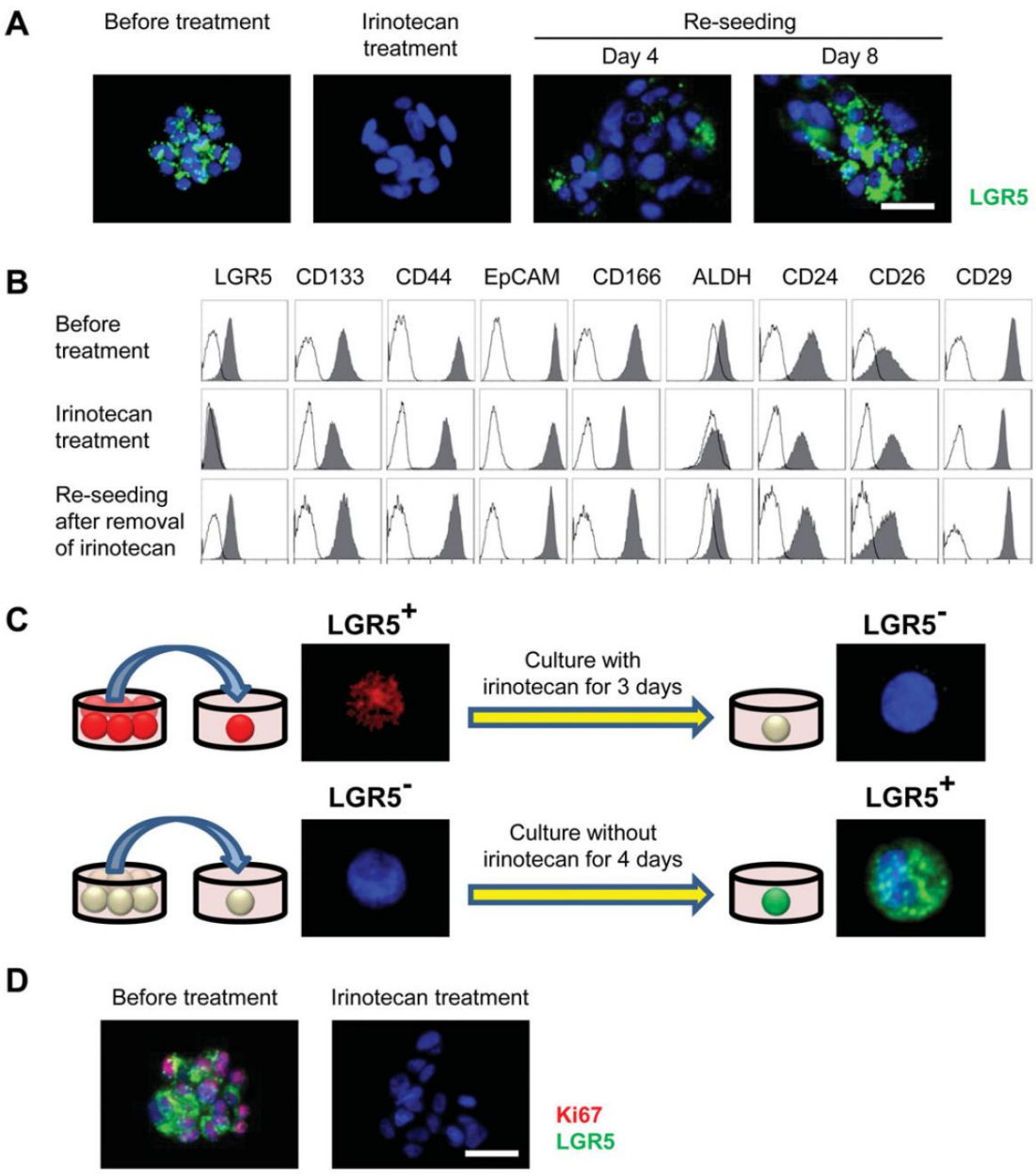

Figure 6. Transition of the colon cancer stem cells between LGR5$^+$ and LGR5$^-$ states *in vitro*.

(A): Immunostaining of LGR5 after treatment of the LGR5$^+$ cells with irinotecan. The adherent LGR5$^+$ cells from PLR123 xenografts cultured in the presence of irinotecan

became LGR5$^-$. The drug-resistant LGR5- cells were re-seeded and further cultured in the absence of irinotecan for the indicated days. The LGR5$^+$ cells appeared 4 days after the reseeding and increased by 8 days. Bar = 50 μm. **(B)**: Expression of CSC markers. The LGR5$^+$ cells from the adherent cultures from PLR123 xenografts before (top) and after treatment with irinotecan (middle) were analyzed by flow cytometry. Cells reseeded after irinotecan treatment (bottom) were also analyzed. Shadow, Fluorescent intensities after staining with the indicated antibodies or ALDH activity; Open, Fluorescent intensities after staining with control isotype antibody or ALDH activity with an ALDH inhibitor. **(C)**: Interconversion of the LGR5$^+$ and LGR5$^-$ states *in vitro*. LGR5$^+$ cells collected by flow cytometry were seeded by limiting dilutions and cultured under an adherent culture condition in the presence of irinotecan for 3 days. Drug-resistant LGR5$^-$ cells that had been treated with irinotecan were seeded by limiting dilutions and cultured under an adherent culture condition for 4 days. The cells were stained with anti-LGR5 antibody to confirm the expression of LGR5. LGR5 was visualized by R-phycoerythrin (PE) -labeled anti-mouse IgG (red) or by AlexaFluor 488-labeled anti-mouse IgG (green). **(D)**: Ki67 staining of the LGR5$^+$ and drug-resistant LGR5$^-$ cells. *In vitro* cultures of the LGR5$^+$ cells and the drug-resistant LGR5$^-$ cells

obtained by the treatment of the adherent $LGR5^+$ cells with irinotecan were double stained with the anti-LGR5 antibody and an anti-Ki67 antibody. Bar = 50 μm.

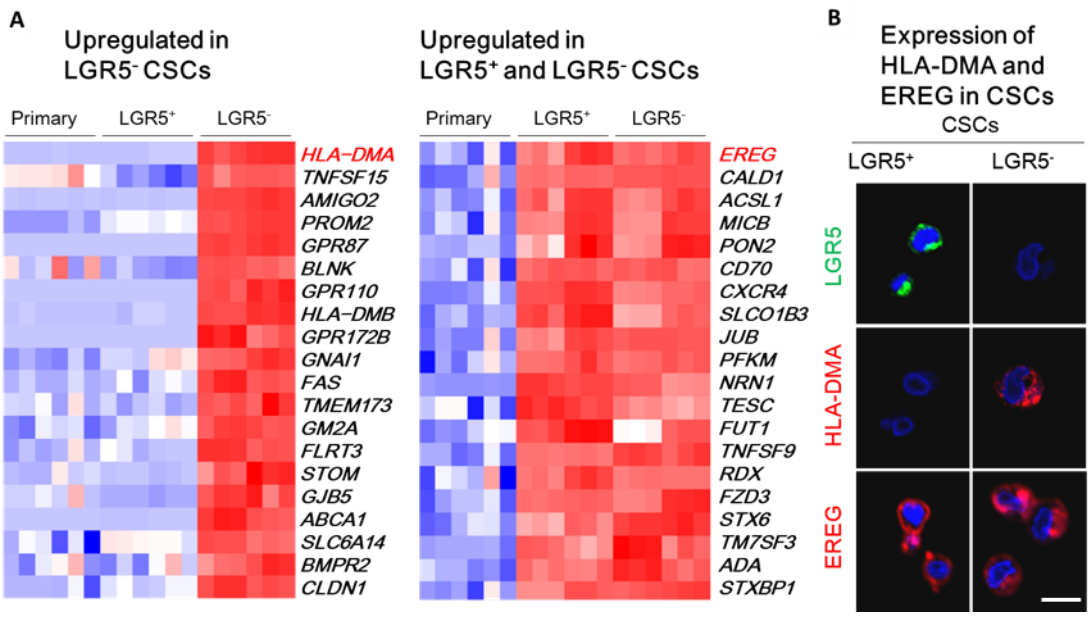

Figure 7. Identification of specific marker for drug resistant LGR5$^-$ cells

(A): DNA microarray. RNA prepared from the primary cells from xenografts, LGR5$^+$ cells, and drug-resistant LGR5$^-$ cells derived from PLR59 and PLR123 were analyzed by Affymetrix U133. Heat map of 20 genes whose expression was markedly upregulated in the drug-resistant LGR5$^-$ cells as compared to the LGR5$^+$ cells (left), and that of 20 genes whose expression was increased in both LGR5$^+$ and drug-resistant LGR5$^-$ cells as compared to the primary cells from the xenografts (right) are shown. Blue colour represents low expressed genes and red colour represents highly expressed genes. **(B)**: Expression of HLA-DMA and EREG in LGR5$^+$ and drug-resistant LGR5$^-$ cells. The LGR5$^+$ (left) and drug-resistant LGR5$^-$ cells (right) derived from PLR123

xenografts were stained with anti-LGR5 antibody (top), anti-HLA-DMA antibody (middle), and anti-EREG antibody (bottom). Bar = 10 μm.

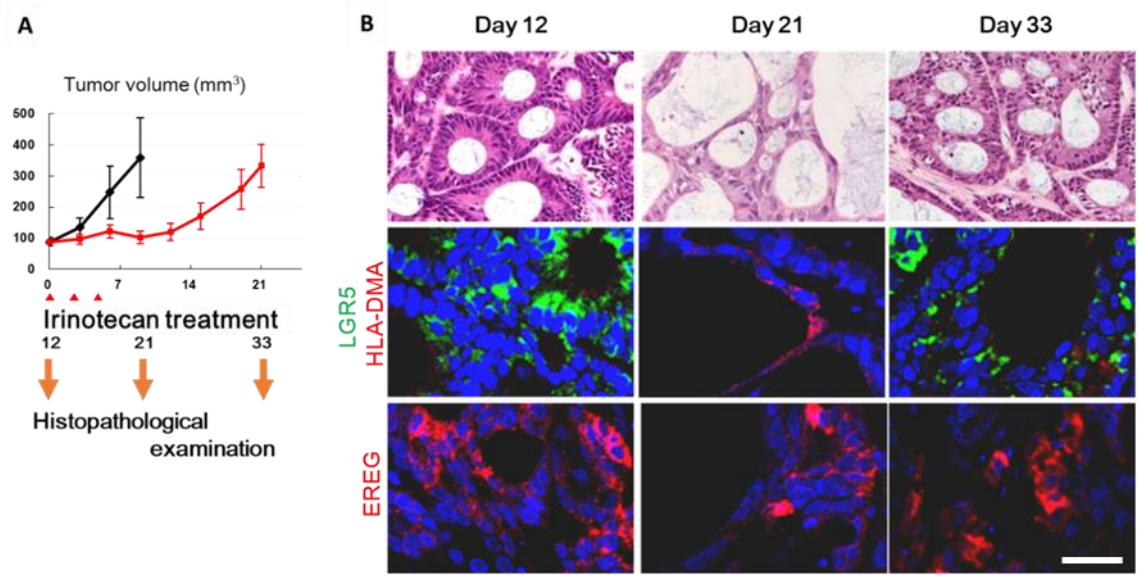

Figure 8. Identification of drug-resistant LGR5$^-$ cells and transition of the colon cancer stem cells between LGR5$^+$ and LGR5$^-$ states *in vivo*.

(A): Tumor volume of the xenografts. The LGR5$^+$ cells of PLR123 were subcutaneously injected into NOG mice, and the mice were administered irinotecan (120 mg/kg per day) 12, 15, and 18 days after the inoculation of the tumor cells. The tumor volume of the control mice (black line) and that of the mice which received irinotecan (red line) are shown. Each value represents mean ± SD (n = 5). **(B)**: Histology and immunostaining for LGR5, HLA-DMA, and EREG of the tumors after treatment of irinotecan. Sections of the xenografts in (A) were excised from the mice at the indicated days after the inoculation of the LGR5$^+$ cells and stained with H&E, anti-LGR5 antibody, anti-HLA-DMA antibody, or anti-EREG antibody. Bar = 25 μm.

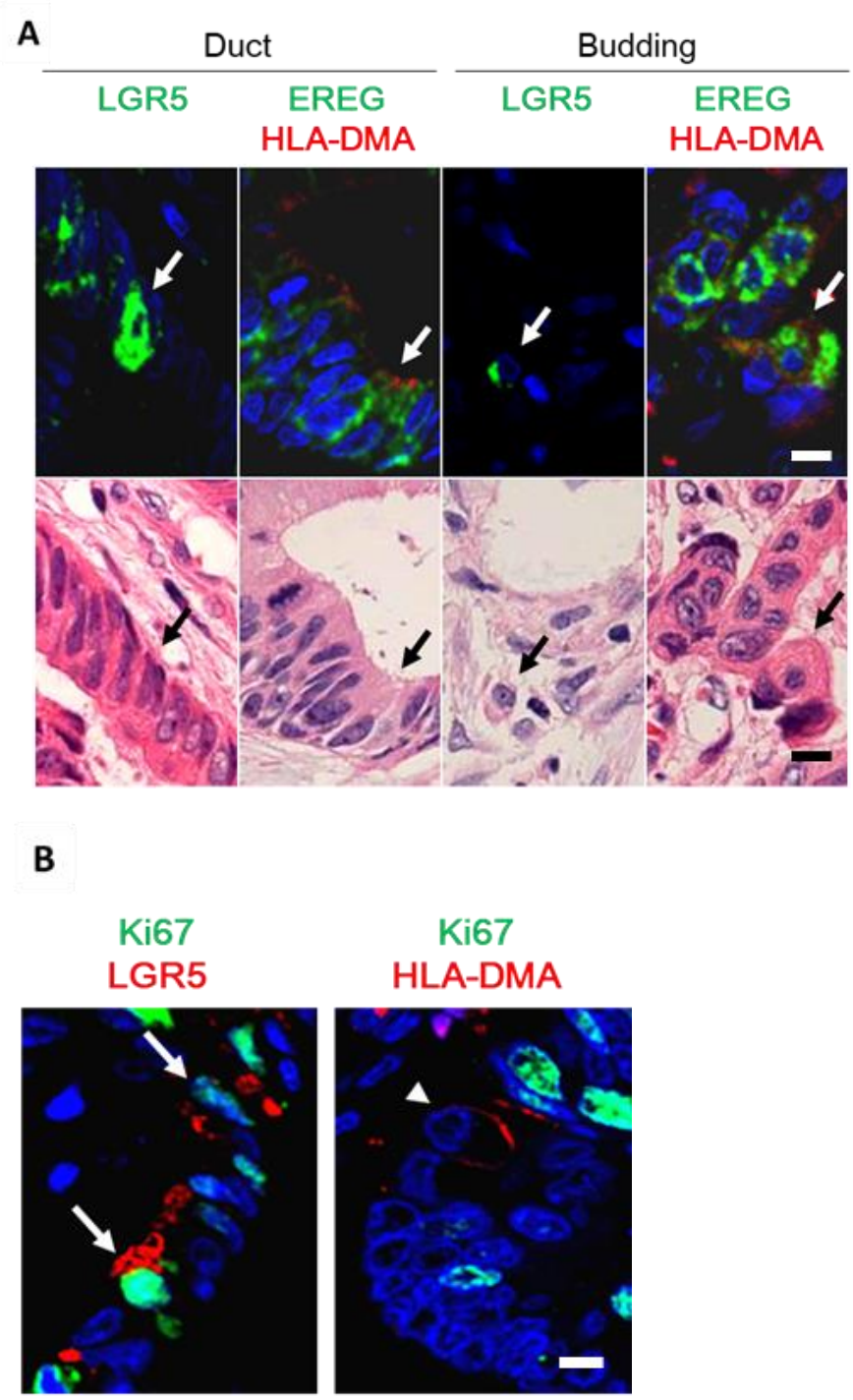

Figure 9. Presence of LGR5^{+} and LGR5^{-} cells in colon cancer and liver metastatic colon cancer from patients.

(A): The same section of the primary colon cancer tissues from patients was stained with H&E or antibodies against LGR5, HLA-DMA, and EREG. $LGR5^+$ and $EREG^+$/$HLA\text{-}DMA^+$ cells are detected in both ductal structures and budding areas of the primary and liver metastatic tumors. $LGR5^+$ cells present as single cells are also found in the interstitium. Similar staining patterns were observed in several tumor tissues from different patients. Arrows indicate typical $LGR5^+$ cells, and arrow heads indicate typical $LGR5^-$/$EREG^+$/$HLA\text{-}DMA^+$ cells. Bar = 10 μm. **(B)**: Ki67 staining of the $LGR5^+$ and the $HLA\text{-}DMA^+$ cells in colon cancer tissues from patients. The sections of the primary colon cancer tissues from patients in (A) were double stained with an anti-Ki67 antibody and anti-LGR5 antibody or anti-HLA-DMA antibody. Arrows: $LGR5^+$/$Ki67^+$ cells, Arrow head: $HLA\text{-}DMA^+$/$Ki67^-$ cells. Bar = 10 μm.

Chapter 2: Alleles of *Insm1* determine whether RIP1-Tag2 mice produce insulinomas or nonfunctioning pancreatic neuroendocrine tumors

Abstract

The two most common types of pancreatic neuroendocrine tumors (PanNETs) are insulinomas and nonfunctioning PanNETs (NF-PanNETs). Insulinomas are small, rarely metastatic tumors that secrete high amounts of insulin, and nonfunctioning PanNETs are larger tumors that are frequently metastatic but which do not secrete hormones. Insulinomas are modeled by the highly studied RIP1-Tag2 (RT2) transgenic mice when bred into a C57Bl/6 (B6) genetic background (also known as RT2 B6 mice). But there has been a need for an animal model of nonfunctioning PanNETs, which in the clinic are a more common and severe disease. Here I show that when bred into a hybrid AB6F1 genetic background, RT2 mice make nonfunctioning stem cell type PanNETs. Compared to insulinomas produced by RT2 B6 mice, the tumors produced by RT2 AB6F1 mice were larger and more metastatic, and the animals did not suffer from hypoglycemia or hyperinsulinemia. Insm1, a beta cell transcription factor, was highly expressed in human insulinomas but unexpressed in other types of PanNETs due

to promoter hypermethylation. *Insm1*-deficient human cell lines expressed stem cell markers, were more invasive *in vitro*, and metastasized at higher rates *in vivo* when compared to isogenic *Insm1*-expressing cell lines. These data demonstrate that expression of *Insm1* can be used to identify whether a PanNET is a localized insulinoma or a metastatic stem cell type tumor.

Introduction

Neuroendocrine cells function by secreting hormones as a reaction to neurological or metabolic stimuli. Insulin-producing beta cells in the pancreas are the best known example of neuroendocrine cells, as beta cell abnormalities can cause diabetes. Neuroendocrine cells are also found in many other places in the body, including the pituitary gland, thyroid, parathyroid, small intestine and large intestine. In order to maintain the right hormonal balance, neuroendocrine cells are subjected to strict growth regulation. However, neuroendocrine cells can transform into neuroendocrine tumors. The transformation of pancreatic beta cells results in PanNETs. PanNETs are the second most common tumors in the pancreas, with an incidence of 1 in 200,000, and the incidence of PanNETs increased (Kuo and Salem, 2013). PanNETs often metastasize to the liver.

For such a rare disease, PanNETs have been a surprisingly popular field of research for tumor biologists. This is explained in part by the fact that PanNETs are produced by the tumor model RIP1-Tag2 (RT2), which was one of the very first transgenic mouse models for cancer (Hanahan, 1985). PanNETs occur in RT2 mice due to the expression of the SV40 T-antigen oncoprotein (Tag) from a rat insulin promoter (RIP). Tumor formation in RT2 mice is rapid and highly reproducible, which facilitates

the testing of both potential therapeutics and potential tumor genes. RT2 is also a rare example of a mouse model that has been validated pharmacologically. Sunitinib and rapamycin have been shown to block tumor growth in RT2 mice (Chiu et al., 2010, Olson et al., 2011) and have subsequently been tested in clinical trials (Yao et al., 2011, Raymond et al., 2011) and were approved by the FDA for use in patients.

Liver metastasis found in patients with PanNETs can also be detected in RT2 mice, although the frequency of metastasis is generally low. Researchers have published many reports on genes that can increase the rate of metastasis in this mouse, including *Igf1r*, *Alk*, *Rhamm*, *Met*, *Bclx*, and *C5* (Sennino et al., 2011, Raymond et al., 2011, Yao et al., 2011, Contractor et al., 2016, Chun et al., 2010, Choi et al., 2011, Lopez and Hanahan, 2002, Du et al., 2011). Also, *Csf1* has been shown to be a metastasis suppressor in RT2 mice (Pyonteck et al., 2012).

Clinically, metastasis is correlated with whether PanNET produces insulin. PanNETs producing insulin are called insulinomas and these tumors are rarely malignant or metastatic; conversely, non-insulin-producing PanNETs are often highly malignant and metastatic (Anderson and Bennett, 2016). Most of the non-insulin-producing PanNETs are “nonfunctioning” PanNETs, so-named because they do not overproduce any of the major pancreatic endocrine hormones (Anderson and Bennett,

2016). It has been estimated that about 85% of PanNETs are nonfunctioning, 10% are insulinomas, and the remaining tumors express other hormones such as gastrin or glucagon. Patients with nonfunctioning PanNETs have a 5-year survival rate of only 33% (Franko et al., 2010), whereas patients with insulinomas rarely die of their disease. Nonfunctioning tumors are also larger in size than insulinomas.

Here I demonstrate that the RT2 mouse model is capable of modeling both insulinomas and NF-PanNETs, with the specific disease depending on the genetic background of the animal. In a hybrid AB6F1 genetic background, low expression levels of a beta cell transcription factor, *Insm1*, favors the development of nonfunctioning stem cell type tumors, whereas in a C57Bl/6 genetic background, higher expression of *Insm1* favors the development of insulinomas. The amount of *Insm1* are correlated with insulin production and with lack of metastasis, in both mice and patients.

Materials and Methods

Human and mouse experiments

Human pancreatic neuroendocrine tumors were provided by the Cooperative Human Tissue Network (CHTN), which obtained informed consent from patients. Human experiments were approved by the Institutional Review Board of CHTN. Mouse experiments were approved by the Institutional Animal Care and Use Committee of Rutgers University. RT2 B6 mice were obtained from the National Cancer Institute (Frederick, MD) and bred to C57Bl6/J (Jackson laboratories) for more than 10 generations. A/J mice were purchased from Jackson Laboratories. Mouse husbandry, euthanasia, and autopsy protocols have been previously described (Contractor et al., 2016). *Insm1* genotypes were not assayed until long after the mice had been euthanized and the metastasis and tumor size data were collected. An ELISA kit for mouse insulin was purchased from RayBiotech and used as recommended by the manufacturer. Serum glucose was measured using a ReliOn Confirm glucose meter and ReliOn Micro Plus test strips.

Cell lines

The QGP1 cell line was purchased from the Japan Health Sciences Foundation. The CM cell line was a gift from the lab of Paolo Pozzilli. CM and QGP1 were grown

in RPMI media (Thermofisher) supplemented with 10% fetal bovine serum (Sigma-Aldrich) at 37 °C under 5% CO_2. To decrease heterogeneity, the cell lines were cloned from single colonies before use.

CM cells were engineered to express human *Insm1* by using lipofectamine 2000 (Thermofisher) to transfect a plasmid expressing the human gene under control of the CMV promoter (Origene); *Insm1*-expressing cells were cloned from single transfectants. QGP1 was engineered to express luciferase, and then *Insm1* was knocked out by CRISPR, using an EDIT-R lentivirus purchased from Dharmacon (source clone identification number VSGHSM_26789438). Potential low expressers were cloned, and characterized by RTPCR and by western blotting, using an Insm1 antibody that was a generous gift from Mark Magnuson. Antisera against β-actin (part number A2228) were purchased from Sigma. Genomic DNA from low *Insm1*-expressing clones was subjected to PCR using primers 5′-CAGGTGTTCCCCTGCAAGTA and 5′-CCCAGACAACAGTTCAAGGC; the PCR products were cloned using the TOPO TA system (Thermofisher), and 12 of the PCR clones were sequenced to confirm the presence of frameshift mutations within the *Insm1* sequence targeted by the EDIT-R lentivirus. QGP1 clone H10 showed two new alleles of *Insm1*, each of which had frameshifting mutations: loss of two nucleotides, CCCGGCctTACGCG, or loss of a

single nucleotide, CCCGGCcTTACGCG. *Insm1* siRNAs si-5, si-6, and si-7 were purchased from Dharmacon, and catalog numbers were J-006535-05-002, J-006535-06-002, and J-006535-07-002, respectively.

Invasion assay

A matrigel-coated invasion chamber with 8 μm pore size (Corning 354480) was used for invasion assays; 20% fetal bovine serum in the upper chamber was used as a chemo-attractant.

Three-dimensional cell culture

Three-dimensional growth of cell lines was performed by mixing 1000 cells with 50 μl of matrigel (Corning 354234), and seeding 5 μl of this mixture into 96-well plates. After 5 min, 200 μl of RPMI/10% FBS media were added and the cells were cultured under CO_2 at 37 °C for 2 weeks.

Metastasis assay

QGP1 cell line expressing luciferase were injected into the left ventricles of nude mice, as previously described (Choi et al., 2016). The day after surgery, and weekly thereafter, mice were sedated with isofluorane, injected with luciferin, and imaged using an IVIS machine. Three weeks after injection, the mice were euthanized by CO_2 asphyxiation and cervical dislocation, and autopsied for metastatic lesions.

Organs were examined visually for metastatic lesions. Three organs (liver, pancreas, and both lungs) were also removed, treated with luciferin, and imaged using an IVIS machine. To assay serum insulin and serum glucose, mice were moved to fresh cages with water bottles but no food for 8 h.

Flow cytometry analysis and cell sorting

Cells were incubated with PE-labeled CD44 antibody (Biolegend, IM7) and 7-AAD Viability Dye (Beckman Coulter). Activity of aldehyde dehydrogenase was determined with AldeFluor Kit (Stem cell Technologies). Flow cytometry analysis and cell sorting were performed using a Cytomics FC500 Flow Cytometer (Beckman Coulter) or a BD Influx High Speed Cell Sorter (BD Biosciences). The purity of sorted cells was >95%.

Analysis of RNA and protein

Fresh-frozen tumor tissues from male mice were minced in Trizol (Thermofisher) and homogenized using a Polytron 1200E. Chloroform was then added and the upper aqueous phase was removed after microcentrifugation at 14,000 r.p.m. RNA was then isolated using an RNAeasy column (Qiagen) as recommended by the manufacturer. RNA was converted to cDNA using reverse transcription reagents (Thermofisher). Real-time RTPCR was then performed, using a Prism 7500 (Applied

Biosystems). Most of the RNAs were measured using pre-designed Taqman assays, which were purchased from Thermofisher. The primers were designed with Primer3 (http://bioinfo.ut.ee/primer3/) and run with SYBR green reagents (Thermofisher): mouse Slc24a3 (5′-CCCTCTGGCAAACTGGAAAC and 5′-GGGATCCCTAGTGTGTAGCC); mouse Cfap61 (5′-AATCACTACCCTCAGCTGCA and 5′-GCCAAAGAAGCATGACCCAT); mouse Rin2 (5′-AACTCCTGGACCCATCATG and 5′-CATCCGCTGTTGACCTCTTG); mouse Xrn2 (5′-GAGGTCAAGCTCAGATCCCAAA and 5′-GTTCCATGGCAGTAGAGGTTCA); mouse Crnkl1 (5′ AGAGAAGAAAGGTCCAGGCC and 5′-GCTTGAGGTTAGGCTGGTTG); mouse Naa20 (5′-AGGGAAGAATGGCATGGACA and 5′-GCTTGTACATGTTGACGGCA); mouse Nkx2-4 (5′-GCCCCATGAACCTGGAGATT and 5′-CACCTACCACATGCCTCCC); human Rin2 (5′-TCCGCACCATCTCCTGTTTC and 5′-GTCTGGACAAGCGAGGAAGT); mouse Sox9 (5′-TATCTTCAAGGCGCTGCAAG and 5′-CCCCTCTCGCTTCAGATCAA); mouse EHF (5′-GCCCGGCAGAAAGTCTTACT and 5′-TTCCAGTCCGCACACAATGT); mouse FoxJ1 (5′-

CACTCTCATCTGCATGGCCA and 5′-AGGTTGTGGCGGATGGAATT); mouse Kat14 (5′-ACGAGAGGCTGAAACTGACA and 5′-ACGTCCACTTCCTTCCAGAG); mouse Zfp120 (5′-AAGCCCAGAAGTTCCGACAT and 5′-AGCAGCGAGATTCCTGTAGG); mouse GZF1 (5′-CTCAGCGCAATTCCCTGTAC and 5′-GTGAACTGCTTCCCACACTG); and human GZF1 (5′-TCACTCAGAACCACATGCTG and 5′-AATTCCGCTGGGCAAAAGTC.

Immunohistochemistry

For antigen retrieval, slides were boiled for 16 min in 0.93% (v/v) Antigen Unmasking Solution H3301 (Vector Labs), and then slowly cooled to room temperature for 30 min. Primary antibody was guinea pig anti-insulin from Dako (A0564), which was diluted 2000-fold in 10% goat serum/1% BSA. Slides were treated with primary antibody overnight at 4 °C. Secondary antibody was affinity-purified, biotinylated anti-guinea pig IgG from Vector Labs (BA-7000), which was diluted 500-fold in 10% goat serum and 1% BSA. Slides were then treated with Vectastain Elite ABC peroxidase kit (Vector Labs) for 30 min, and with ImmPact DAB peroxidase substrate (Vector Labs SK-4105) for 1 min. The slides were counterstained with hematoxylin (Vector Labs).

Statistical analysis

Graphpad Prism 7.04 software was used for statistical analysis. Two-tailed *t*-test was used to compare RNA expression levels from sets of mouse and human tumors. Fisher's exact test was used to compare metastasis frequencies. Pearson correlation analysis was used to compare Insm1 and Ins1 expression in human tumors. Nonparametric Mann–Whitney analysis was used to evaluate tumor volumes. Outliers were identified by Rout analysis (q = 1%).

Results

RT2 B6 and RT2 AB6F1 mice show profound phenotypic differences

RT2 AB6F1 mice were produced by mating females from the inbred A/J genetic background to male RT2 B6 mice, which have an inbred C57Bl/6 J genetic background (Contractor et al., 2016). For both genetic origins, pancreatic tumors were produced which were confirmed to be neuroendocrine tumors upon pathologic examination, although less well differentiated than the PanNETs found in most patients. There was a difference in the frequency of hepatic metastases in the two genetic backgrounds, metastases being much more frequent in RT2 AB6F1 mice than in RT2 B6 mice (Fig. 10A). Other genetic backgrounds have also been identified to influence the frequency of metastases of RT2 mice (Chun et al., 2010). Primary tumors were larger in RT2 AB6F1 age-paired mice compared with RT2 B6 (Fig. 10B). Remarkably, even with larger metastatic tumors, RT2 AB6F1 mice lived longer than RT2 B6 mice (Fig. 10C). Eighty-five percent of RT2 AB6F1 mice, but only 33% of RT2 B6 mice lived to be 16 weeks old. Early mortality may be associated with hypoglycaemia, which can only be observed in RT2 B6 mice and not in RT2 AB6F1 mice (Fig. 10D). Hypoglycemia was previously reported in RT2 mice, so it was a surprise to discover that RT2 AB6F1 was not hypoglycemic. As a result of their hypoglycaemia, RT2 B6 mice were also very

hyperinsulinemic, with an average nine-fold increase in serum insulin compared to wild-type B6 mice (Fig. 10E). In contrast, despite their larger PanNETs, RT2 AB6F1 expressed only twice as much serum insulin as wild-type AB6F1 mice.

Tumors from RT2 AB6F1 mice profile as stem cell type pancreatic neuroendocrine tumors.

Primary pancreatic tumors from RT2 B6 and RT2 AB6F1 mice were collected and RT2 AB6F1 tumors showed lower levels of mRNAs for insulin, consistent with their low serum insulin levels (Fig. 11A). RT2 AB6F1 mouse tumors also transcribed fewer mRNAs for other beta markers such as *Nkx6-1*, *MafA* and *Pdx1* (Fig. 11A). It is interesting to note that the transcription of the SV40 T-antigen gene did not differ between RT2 AB6F1 and RT2 B6 mouse tumors (Fig. 11B), even when the expression of insulin was significantly different between the two mice. This may reflect the leakiness of the activation of insulin promoter that controls expression of SV40 T-antigen; this transgene has also been shown to express in other insulin-negative neuroendocrine cells from small intestine and pituitary tissue (Biondi et al., 2004, Grant et al., 1991).

With their smaller tumors, low metastasis, hypoglycemia, and hyperinsulinemia, RT2 B6 mice display all the clinical characteristics of human insulinomas. In contrast,

RT2 AB6F1 mice developed another type of PanNET that does not express insulin. In RT2 AB6F1 tumors, glucagon and vasoactive intestinal peptide transcription was not elevated, and PPY and gastrin transcription was reduced, but somatostatin transcription was increased (Fig. 11C). Although elevated, the levels of somatostatin transcription were still low. Patients with somatostatinomas suffer from weight loss and diarrhea, whereas RT2 AB6F1 were slightly overweight and had firm stools. For further characterization, I evaluated the expression of pancreatic stem cell markers such as *Lgr5*, *Sox9*, *FoxJ1*, and *EHF* (Dorrell et al., 2014), and detected high levels of these stem cell markers in tumors of RT2 AB6F1 mice (Fig. 11D). Based on these experiments, I conclude that the tumors produced by RT2 AB6F1 mice are stem cell type PanNETs.

Insm1 regulates tumor differentiation as well as normal pancreas

Of the many genes known to be important for the differentiation of beta cells, Insm1 can lead to the trans-differentiation of pancreatic ductal cells into endocrine cells (Zhang et al., 2010). *Insm1*-knockout mice have also been reported to make beta cells that are deficient in insulin expression (Gierl et al., 2006), which is perhaps similar to the deficient insulin expression in mouse RT2 AB6F1 tumors. Notably, *Insm1* was first isolated as a very highly expressed RNA in insulinomas (Goto et al., 1992). As shown in

Fig. 12A, expression of *Insm1* mRNA was higher in the insulinomas from RT2 B6 and lower in stem cell type tumors from RT2 AB6F1 mice. Insm1 protein levels were also higher in RT2 B6 tumors, as shown by western blot (Fig. 12B). The expression of *Insm1* was characterized in a number of samples taken from patients. As shown in Fig. 12C, the mRNA level of *Insm1* is strongly correlated with the mRNA level of insulin. These experiments suggest that Insm1 might be relevant to the insulinomas.

Loss of *Insm1* expression promotes an invasive stem cell phenotype in human pancreatic neuroendocrine tumor cell line QGP1.

In order to evaluate the function of Insm1 in PanNETs, I confirmed that QGP1 was an Insm1 positive cell line. In Fig. 13A and 13B, the effect of transient knockdown of *Insm1* expression using three different shRNAs was tested in the QGP1 cell line. *Insm1* knockdown increased expression of the so-called Yamanaka factors (Takahashi and Yamanaka, 2006), which are known to increase pluripotency of differentiated cells. Next, CRISPR-Cas9 technology was used to stably knock out *Insm1* from QGP1-TGL cells, a version of QGP1 engineered to express firefly luciferase (Fig. 13C). The *Insm1* knockout increased the number of cells expressing CD44, which is a marker of stem cells (Fig. 13D). The cell lines expressing *Insm1* and *Insm1*-null were then tested for *in vitro* invasiveness using a transwell assay. Invasiveness is a common property of

metastatic cells. For the QGP1 cell line, invasiveness was higher when expression of *Insm1* was absent, indicating that Insm1 is a repressor of invasion (Fig. 13E). In order to test the effect of Insm1 on tumor metastasis, *Insm1*-expressing, or *Insm1*-null QGP1-TGL cells were injected into the left ventricles of immune compromised mice. Images of mice were taken each week for luciferase bioluminescence to evaluate the spread of metastasis. Within two weeks, strong luciferase signals were detected in the torso, which were especially intense in animals injected with *Insm1*-null QGP1. In animal dissection, metastatic lesions were found to be more prominent in the lungs, liver, and pancreas. Overall, there was a 3.3-fold increase in the presence of metastatic tumors in animals injected with *Insm1*-null QGP1-TGL cells (Fig. 13F, 13G). These data indicate that loss of *Insm1* can produce more invasive, stem-like cells.

***Insm1* expression decreases invasiveness of human pancreatic neuroendocrine tumor cell line CM.**

The CM cell line is an Insm1 negative cell line and particularly invasive (Fig. 14A, 14B). The effects of Insm1 on this cell line could be seen in a transwell assay. Although wild type CM cells invaded the surrounding matrix, the CM cells expressing *Insm1* only formed less invasive spheroids (Fig. 14C). In addition, the *Insm1* expression attenuated the signal of the CD44 stem cell marker (Fig. 14D). These data indicate that

gain of *Insm1* can induce the differentiation of PanNETs and decrease their invasiveness.

Together, these cell line experiments show that *Insm1* depletion can lead to stem cell formation, increase invasion, and cause metastasis. Furthermore, these data suggest that the difference between the less metastatic, more differentiated insulinomas of RT2 B6 mice and the stem cell type PanNETs of RT2 AB6F1 mice may be due to differences in *Insm1* expression. Data from cell lines strongly suggest that allelic differences in *Insm1* between A/J and B6 mouse lines lead to different types of neuroendocrine tumors in RT2 mice.

Discussion

Insm1 is a transcription factor that promotes beta cell differentiation (Osipovich et al., 2014), and other tissue-specific differentiation factors have also been shown to suppress metastasis, such as GATA3 in breast tumors (Kouros-Mehr et al., 2008) and NKX2-1 in lung tumors (Winslow et al., 2011). It is widely believed that the loss of these differentiating factors leads to metastasis by causing dedifferentiation to stem cells, and that stem cells increase metastases because they are more invasive and less prone to anoikis (Lawson et al., 2015, Mani et al., 2008, Hermann et al., 2007). In the present study, expression of the stem cell marker was increased in RT2 AB6F1 mice with low *Insm1* expression. In addition, removal of *Insm1* from the QGP1 cell line resulted in increased stem cell markers, increased invasiveness, and increased metastasis. These results indicate that deletion of *Insm1* transforms the cancer cells into a stem cell type with high metastatic potential.

The sub-types of PanNETs that may occur in patients exhibit significant clinical differences, as non-functional stem cell type PanNETs are more common and result in worse outcomes than insulinomas (Franko et al., 2010). The understanding of how different subtypes of tumors occur has been an active field of research. In animal models for breast and brain tumors, it has been shown that some oncogenic mutations or

tumor suppressors may promote development of one subtype of tumor over another (Jacques et al., 2010, Liu et al., 2014). In recently published work, mutations in *Men1*, *Daxx*, and *Atrx* have been less common in human insulinomas than in human non-functional stem cell type tumors, suggesting that these types of PanNETs are affected by the presence of these driver mutations (Chan et al., 2018). However, this work also shows that mutations in the tumor suppressor gene are not enough to explain why different tumor subtypes can occur. Using mice that share a common driver oncogene, I have shown that tumor subtypes in the form of different alleles of the *Insm1* gene are also affected by spontaneous genetic diversity. It would be interesting to know if the expression of *Insm1* can be directly influenced by mutations in *Men1*, *Daxx*, and *Atrx* that encode chromatin-remodeling proteins. However, it is also important to point out that mouse models do not always reflect how tumors develop in patients. Indeed, it is not clear if a low expression of *Insm1* is a direct cause of stem cell type PanNETs in patients, or a by-product of the cell type from which these tumors originate (Falchetti, 2017).

In patients, PanNET tumors with stem cell properties are characterized by a high rate of metastasis, which is a major clinical problem. RT2 B6 mice have been used in metastasis studies, but their low metastatic capacity and early death due to

hypoglycemia have been problematic. RT2 AB6F1 mice overcome these problems because they are not hypoglycemic, and metastases are seen earlier and more frequently. The development of the RT2 AB6F1 model is expected to improve our ability to test drugs that can prevent the metastases of PanNET.

Although many drugs have shown anti-metastatic activity in mouse models, there have been no clinical trials designed to test drugs that can reduce the risk of metastasis. This is despite the fact that metastasis is believed to be the cause of nearly all cancer deaths. There are several practical reasons for the lack of metastasis trials, including the fact that most clinical trials are conducted on patients in the late stages of their disease after metastasis. However, another problem may be that spontaneous synchronous mouse models of metastasis are rare. For this reason, the RT2 AB6F1 mouse model may be of great value. Cancer in patients with PanNET is often detected before their tumors metastasize, but cancer in patients with non-functional stem cell type diseases develop metastases much earlier. RT2 AB6F1 mice could prove to be an attractive preclinical model for developing and testing clinically relevant anti-metastatic agents.

Figures

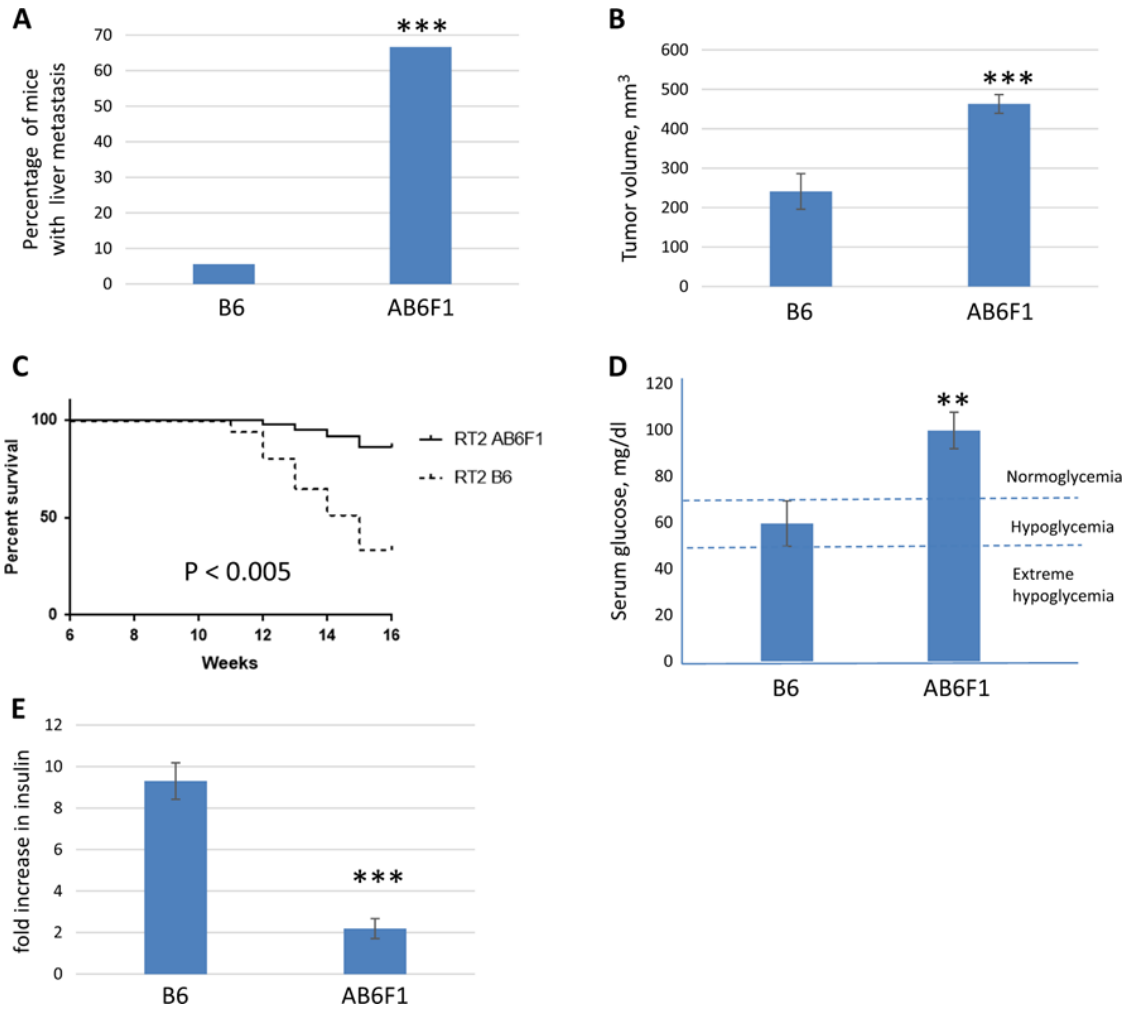

Figure 10. RT2 B6 and RT2 AB6F1 mice show profound phenotypic differences.

(A): Percentage of 15-week-old RT2 mice with liver metastasis, by genetic background. All mice were males, and 18 mice from each lineage were analyzed. Statistical significance was determined using Fisher's exact test. B6 mice have the C57Bl/6 genetic background, and AB6F1 mice are hybrids resulting from mating female A/J mice to male C57Bl/6 mice. **(B):** Volume of primary pancreatic tumors according to the genetic background. All mice were 17-week-old males; 24 RT2 B6 mice and 138 RT2

AB6F1 mice were analyzed. Statistical significance was determined using Mann–Whitney test. **(C):** Kaplan–Meier survival curves for RT2 mice between 6 and 16 weeks of age according to the genetic background. **(D):** Eight hours after removal of food, serum glucose was measured in RT2 mice of different genetic backgrounds. All mice were males and 12-13 weeks old. Fifteen RT2 AB6F1 and 12 RT2 B6 were analyzed. Statistical significance was determined using two-tailed *t*-test. **(E):** RT2 mice or wildtype littermates were held without food for 8 h, then serum insulin was measured and compared to that of littermates (B6 or AB6F1) lacking the SV40 T-antigen transgene. Mice were males and 13 weeks old. Nine and 11 RT2 B6 and RT2 AB6F1 mice were measured, respectively. Statistical significance was determined using two-tailed *t*-test.

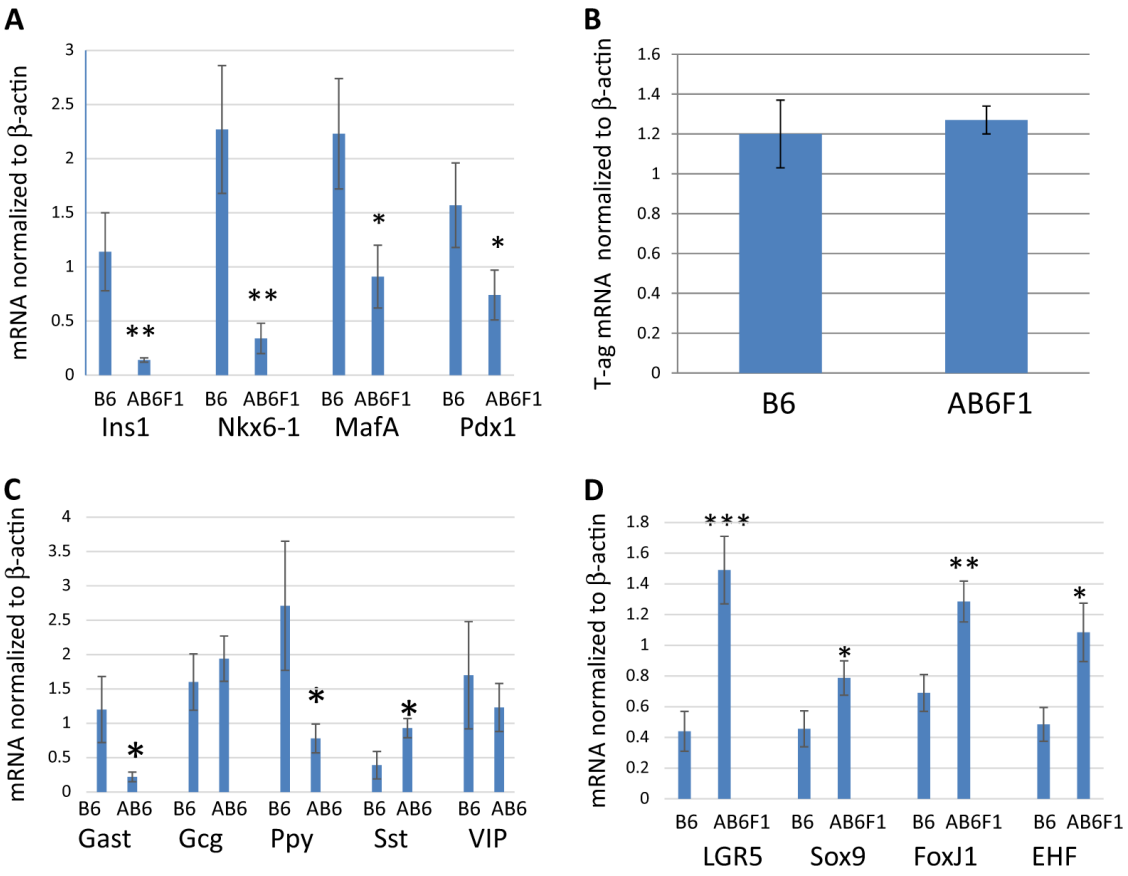

Figure 11. Tumors from RT2 AB6F1 mice profile as nonfunctioning pancreatic neuroendocrine tumors.

In each figure, Q-PCR was used to measure gene expression using cDNA prepared from primary tumors isolated from 17 male RT2 B6 mice and from 25 male RT2 AB6F1 mice. All statistical analysis was performed using two-tailed *t*-test. **(A):** Beta cell markers insulin-1 (*Ins1*), *Nkx6-1*, *MafA*, and *Pdx1*. **(B):** SV40 T-antigen, which is the oncogene that drives tumorigenesis in RT2 mice. **(C):** Pancreatic neuroendocrine hormones gastrin (Gast), glucagon (Gcg), pancreatic polypeptide (Ppy), somatostatin

(Sst), and vasoactive intestinal peptide (Vip). **(D):** Pancreatic stem cell markers *Lgr5*, *Sox9*, *FoxJ1*, and *EHF*.

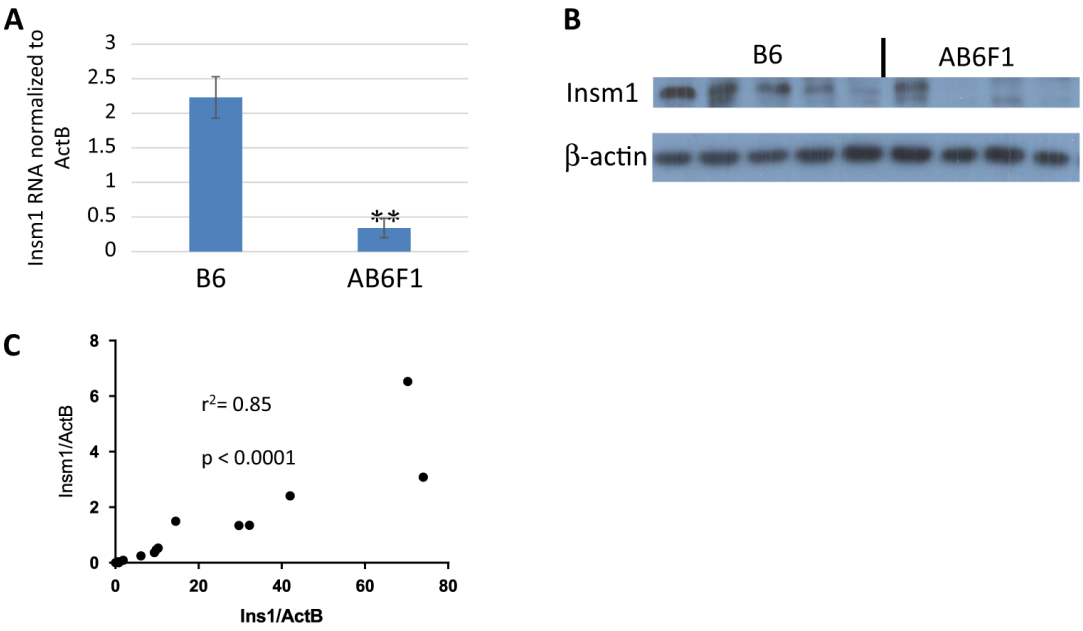

Figure 12. Insulinomas from humans and mice express high levels of transcription factor *Insm1*.

(A): Q-PCR analysis of *Insm1* expression from primary tumors isolated from 17 male RT2 B6 mice or from 25 male RT2 AB6F1 mice. Statistical significance was determined using two-tailed *t*-test. **(B):** Western blot analyses of Insm1 and β-actin expression from pancreatic neuroendocrine tumors of RT2 B6 or RT2 AB6F1 mice. **(C):** mRNA and cDNA were prepared from 39 human pancreatic neuroendocrine tumors, and transcription of beta cell markers Ins1 and *Insm1* was assayed by Q-PCR. Most of the tumors occupy the (0,0) point of the graph. Statistical analysis was performed by Pearson correlation.

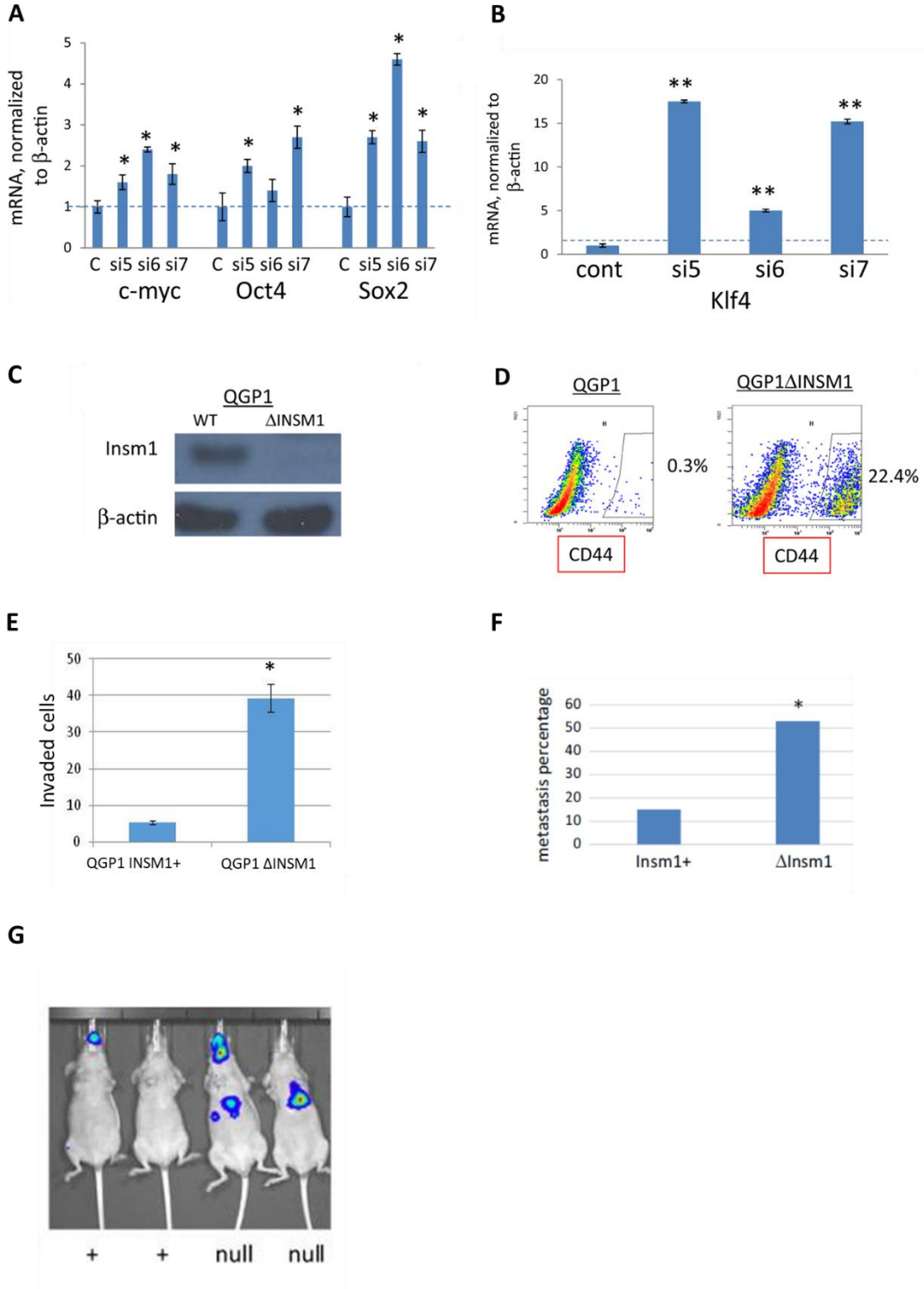

Figure 13. Loss of *Insm1* expression promotes an invasive stem cell phenotype in human pancreatic neuroendocrine tumor cell line QGP1.

(A), (B): The QGP1 cell line was transfected with three different siRNAs directed against *Insm1* (si-5, si-6, or si-7) or with control si-RNA (C, or cont). Eighty-four hours later, transcription of reprogramming genes *Myc*, *Oct4*, and *Sox2* (A) or *Klf4* (B) was measured by Q-PCR. **(C):** Western blot results using an antibody against *Insm1* to measure expression in the QGP1-TGL cell line and in an isogenic version of QGP1-TGL in which the *Insm1* genes were knocked out using CRISPR-Cas9. Sequencing results for the knockout cell line are shown in the Materials and Methods section. **(D):** The QGP1-TGL cell line expressing *Insm1*, as well as QGP1-TGL stably knocked out for the *Insm1* gene, were tested for expression of stem cell markers CD44. **(E):** Transwell assays were used to measure the ability of QGP1 cells to migrate toward 20% serum across a membrane with 8 μm pores, and then to invade matrigel. **(F):** Quantitation of metastases from lung, pancreas, and liver, which were isolated from 14 mice treated with luciferase-expressing QGP-TGL cells that either express or cannot express *Insm1*. Metastasis was arbitrarily defined as individual organs giving radiance readings above 10^5 photons/s/cm2/steradian following luciferin treatment. Statistical significance was determined using Fisher's exact test. **(G):** Representative image of Figure (F). Two mice on the left were injected with cells that express Insm1 (+), and the other animals were injected with cells unable to express Insm1 (null).

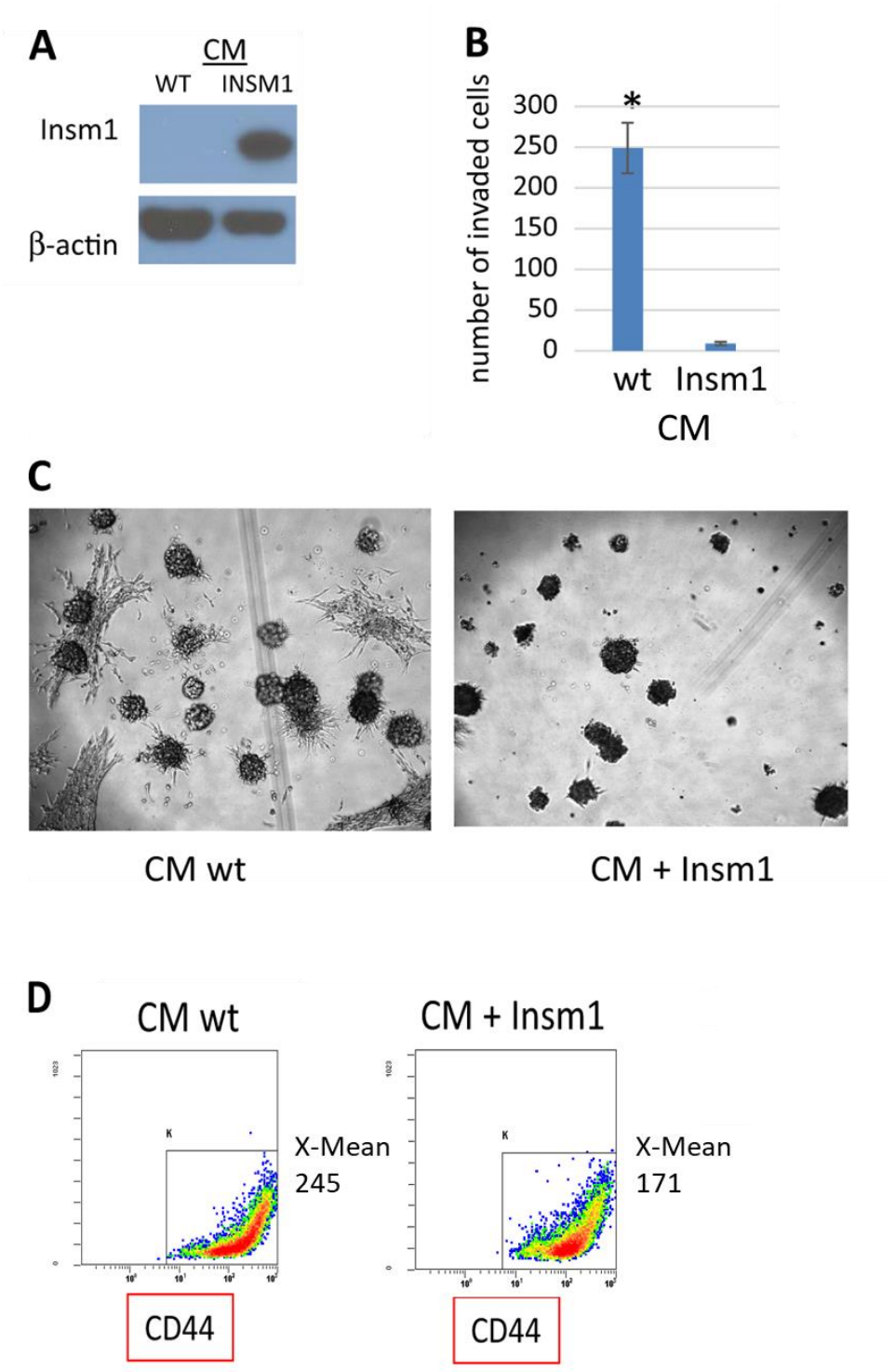

Figure 14. ***Insm1*** **expression decreases invasiveness of human pancreatic neuroendocrine tumor cell line CM.**

(A): Western blot analysis using antisera against Insm1 or β-actin to analyze protein extracts from isogenic pairs of CM cells. CM cells do not normally express *Insm1*, so a plasmid expressing *Insm1* under control of the CMV promoter was introduced and a clone physiologically expressing *Insm1* was isolated. **(B):** Transwell assays were used to measure the ability of CM cells to migrate toward 20% serum across a membrane with 8 μm pores, and then to invade matrigel. **(C):** Single cells of the highly invasive CM cell line were grown into three-dimensional colonies for 2 weeks in matrigel. The presence of Insm1 changes the morphology of the colonies, decreasing their invasiveness and turning them spheroid. **(D):** The CM wild type cell line as well as CM cell line expressing *Insm1* were tested for expression of stem cell markers CD44.

General discussion

In this study, I have shown that LGR5 and Insm1, which function in normal stem cells, maintain their functions in cancer and regulate stemness. In colorectal cancer, $LGR5^+$ cells self-renewed and actively proliferated. In addition, $LGR5^+$ cells had a strong ability to form tumors that maintained a hierarchical structure. This is the first report showing that LGR5 can be used as a CSC marker. In normal cells, the LGR5 ligand R-spondin activates the WNT pathway for self-renewal by binding to LGR5, and similarly, established $LGR5^+$ cell lines were also found to self-renew by adherent culture with R-spondin. These results indicate that stemness is maintained in cancer cells by a mechanism similar to that in normal cells. Furthermore, it was found that $LGR5^+$ cells changed to $LGR5^-$ cells upon anticancer drug treatment and ceased to self-renew. In drug-resistant cells, the expression of LGR5 and the proliferation marker Ki67 was down-regulated, suggesting that CSCs in the drug environment inactivate the WNT pathway and become non-proliferative. Interestingly, in situations where drugs were excluded, $LGR5^-$ cells were found to re-express LGR5 and proliferate again. In contrast, no such changes were observed in commercially available cell lines other than the CSC cell line. The mechanism of drug resistance regulating the expression of LGR5

was found to be CSC specific. A variety of drugs targeting the WNT pathway are currently under development (Jung and Park, 2020, Zhong and Virshup, 2020). This study shows that these drugs can be developed to mitigate drug resistance and recurrence of colorectal CSCs and can potentially improve cancer treatment.

$LGR5^-$ cells were found to have the important function of drug resistance, but their molecular mechanism remains unclear. Recently, it has been reported that LGR5 expression is inhibited by p53 (Ma et al., 2019, Pak et al., 2020), and indeed, in this study, I found an increase of p53 in $LGR5^-$ cells. p53 has been identified as a tumor suppressor gene and its mutation is known to be strongly involved in cancer development. It has also been reported that stressors may control the gain of function of p53 and that mutant p53-depedent signaling determines the fate of cells (Amelio and Melino, 2020). In CSCs, external stresses such as anticancer drug treatment may activate p53, which suppresses LGR5 expression and inactivates the WNT pathway, inducing the cancer to become drug resistant.

The intestinal epithelium has the ability to regenerate rapidly to survive acute injury and regain function. In models of radiation injury, $LGR5^+$ stem cells and damage-resistant spare stem cells have been shown to be present (Barker, 2014). Under stress conditions such as radiation, $LGR5^+$ cells disappear and $LGR5^-$ cells survive. Once the

stress is removed, extracellular niche stimulation produces $LGR5^+$ cells from $LGR5^-$ cells. In normal cells, it has been discussed as a cellular plasticity. This phenomenon also explains the drug resistance mechanism of CSCs found in this study. In CSC plasticity, differentiated cells reportedly transform into CSCs via epithelial-mesenchymal transition (EMT). EMT is a highly conserved cellular process that transforms epithelial cells into mesenchymal cells and is known to be associated with cancer progression, metastasis, and drug resistance (Gupta et al., 2011). In this study, I identified EREG as a factor present in both $LGR5^+$ and $LGR5^-$ cells. EREG is one of the members of the EGF family and activates the EGFR signal and EMT (Wang et al., 2019). EREG may have an important function in colon cancer plasticity.

In addition to drug resistance, metastasis is also an important clinical problem in cancer treatment. In this study, PanNETs that do not express Insm1 were shown to be stem cell type cancers and to have a high metastatic potential. In normal tissues, Insm1 is known to be involved in the trans-differentiation of aciner cells to beta cells (Zhang et al., 2012) and the trans-differentiation of outer hair cells to inner hair cells (Wiwatpanit et al., 2018) by regulating downstream gene expression. Furthermore, in the absence of *Insm1*, pancreatic endocrine cells have many characteristics of progenitor cells and highly express EMT markers, *Notch*, *Tgf*, *Bmp*, and *Wnt* genes (Osipovich et al., 2014).

In pancreatic cancer, the present study shows that reduction of Insm1 causes cancer cells to acquire CSC properties and increases their invasion and metastatic capacity. This change is also indicative of cancer plasticity. As in normal cells, *Insm1* depletion may activate EMT and induce the transformation of endocrine cancer cells into CSCs. In clinical cancers, the prognosis of non-functional stem cell cancers is poor, and detailed analysis of this Insm1 repression mechanism and cancer plasticity may enable the development of drugs to prevent the malignant transformation of cancer.

In this study, I present new biological insights into drug resistance and metastasis in cancer by focusing on functions that are also present in normal stem cells. The heterogeneity and stem cell involvement in cancer have long been the focus of attention, and recent technological advances in flow cytometry and the use of transgenic mice have led to a dramatic increase in CSC research. However, at the same time that the CSC field is becoming more active, many papers that do not precisely understand the definition of stem cell nature have been recognized. The need for an accurate discussion of stem cell nature is therefore being debated (Kreso and Dick, 2014). By focusing on normal stem cells, Fumagalli and his colleagues recently found that many of the metastases of colorectal cancer are seeded by $Lgr5^-$ cells, which have the inherent ability to become $Lgr5^+$ CSCs and form an epithelial hierarchy of metastatic tumors

(Fumagalli et al., 2020). Their work and this study reveal that LGR5$^-$ cells exhibit important functions with respect to drug resistance as well as metastasis, suggesting that focusing on molecules associated with normal stem cells is very important for understanding the mechanisms of drug resistance, recurrence, and metastasis in cancer. Cancer is the leading cause of mortality, but we have yet to develop a cure. The findings of this research could provide new insights into drug resistance and metastasis and contribute to the development of more effective drugs.

Acknowledgements

I am deeply grateful to Professor Tomoki Chiba at University of Tsukuba for guiding my work and for his valuable discussions during my doctoral program.

I would like to thank Dr. Osamu Natori, Dr. Masaki Yamazaki, Dr. Shinichi Funahashi Ms. Yu Jau Chen, Ms. Tanupriya Contractor and Mr. Richard Clausen for their valuable suggestions, contributions and helpful supports, and Dr. Tatsumi Yamazaki, Dr. Hisafumi Okabe, Dr. Koichi Matsubara, Dr. Masami Suzuki, Dr. Atsuhiko Kato, Dr. Arnold J Levine, Dr. Chris R Harris and Dr. Evan Vosburgh for their brilliant insights.

Finally, I would like to thank my family for supporting for everything they do for me.

References

Al-Hajj M, Wicha MS, Benito-Hernandez A, Morrison SJ, Clarke MF. (2003). Prospective identification of tumorigenic breast cancer cells. Proc Natl Acad Sci U S A. 100:3983-8.

Amelio I, Melino G. (2020). Context is everything: extrinsic signalling and gain-of-function p53 mutants. Cell Death Discov. 6:16.

Anderson CW, Bennett JJ. (2016). Clinical presentation and diagnosis of pancreatic neuroendocrine tumors. Surg. Oncol. Clin. N. Am. 25:363-374.

Barker N, van Es JH, Kuipers J, Kujala P, van den Born M, Cozijnsen M, Haegebarth A, Korving J, Begthel H, Peters PJ, Clevers H. (2007). Identification of stem cells in small intestine and colon by marker gene Lgr5. Nature. 449:1003-7.

Barker N, Ridgway RA, van Es JH, van de Wetering M, Begthel H, van den Born M, Danenberg E, Clarke AR, Sansom OJ, Clevers H. (2009). Crypt stem cells as the cells-of-origin of intestinal cancer. Nature. 457:608-11.

Barker N, Bartfeld S, Clevers H. (2010). Tissue-resident adult stem cell populations of rapidly self-renewing organs. Cell Stem Cell. 7:656-70.

Barker N. (2014). Adult intestinal stem cells: critical drivers of epithelial homeostasis and regeneration. Nat Rev Mol Cell Biol. 15:19-33.

Baylin SB, Weisburger WR, J Eggleston JC, Mendelsohn G, Beaven MA, Abeloff MD, Ettinger DS. (1978). Variable content of histaminase, L-dopa decarboxylase and calcitonin in small-cell carcinoma of the lung. Biologic and clinical implications. N Engl J Med. 299:105-10.

Bennett DC, Peachey LA, Durbin H, Rudland PS. (1978). A possible mammary stem cell line. Cell. 5:283-98.

Biondi CA, Gartside MG, Waring P, Loffler KA, Stark MS, Magnuson MA, Kay GF, Hayward NK. (2004). Conditional inactivation of the MEN1 gene leads to pancreatic and pituitary tumorigenesis but does not affect normal development of these tissues. Mol Cell Biol. 24:3125-31.

Bonnet D, Dick JE. (1997). Human acute myeloid leukemia is organized as a hierarchy that originates from a primitive hematopoietic cell. Nat Med. 3:730-7.

Burrell RA, McGranahan N, Bartek J, Swanton C. (2013). The causes and consequences of genetic heterogeneity in cancer evolution. Nature. 501:338-45.

Chan CS, Laddha SV, Lewis PW, Koletsky MS, Robzyk K, Da Silva E, Torres PJ, Untch BR, Li J, Bose P, Chan TA, Klimstra DS, Allis CD, Tang LH. (2018). ATRX, DAXX or MEN1 mutant pancreatic neuroendocrine tumors are a distinct alpha-cell signature subgroup. Nat Commun. 9:4158.

Chen C, Notkins AL, Lan MS. (2019). Insulinoma-Associated-1: From Neuroendocrine Tumor Marker to Cancer Therapeutics. Mol Cancer Res. 17:1597-1604.

Chiu CW, Nozawa H, Hanahan D. (2010). Survival benefit with proapoptotic molecular and pathologic responses from dual targeting of mammalian target of rapamycin and epidermal growth factor receptor in a preclinical model of pancreatic neuroendocrine carcinogenesis. J. Clin. Oncol. 28:4425-4433.

Choi S, Chen Z, Tang LH, Fang Y, Shin SJ, Panarelli NC, Chen YT, Li Y, Jiang X, Du YN. (2016). Bcl-xL promotes metastasis independent of its anti-apoptotic activity. Nat Commun. 7:10384.

Chun MG, Mao JH, Chiu CW, Balmain A, Hanahan D. (2010). Polymorphic genetic control of tumor invasion in a mouse model of pancreatic neuroendocrine carcinogenesis. Proc. Natl. Acad. Sci. USA. 107:17268-17273.

Cohnheim J. (1875). Congenitales, quergestreiftes Muskelsarkom der Nieren. Virchows Arch. 65: 64-69.

Collins AT, Berry PA, Hyde C, Stower MJ, Maitland NJ. (2005). Prospective identification of tumorigenic prostate cancer stem cells.Cancer Res. 65:10946-51.

Contractor T, Kobayashi S, da Silva E, Clausen R, Chan C, Vosburgh E, Tang LH, Levine AJ, Harris CR. (2016). Sexual dimorphism of liver metastasis by murine pancreatic neuroendocrine tumors is affected by expression of complement C5. Oncotarget. 7:30585-96.

de Lau W, Barker N, Low TY, Koo BK, Li VS, Teunissen H, Kujala P, Haegebarth A, Peters PJ, van de Wetering M, Stange DE, van Es JE, Guardavaccaro D, Schasfoort RB, Mohri Y, Nishimori K, Mohammed S, Heck AJ, Clevers H. (2011). Lgr5 homologues associate with Wnt receptors and mediate R-spondin signalling. Nature. 476:293-7.

Dick JE. (2008). Stem cell concepts renew cancer research. Blood. 112:4793-807.

Dieter SM, Ball CR, Hoffmann CM, Nowrouzi A, Herbst F, Zavidij O, Abel U, Arens A, Weichert W, Brand K, Koch M, Weitz J, Schmidt M, von Kalle C,

Glimm H. (2011). Distinct types of tumor-initiating cells form human colon cancer tumors and metastases. Cell Stem Cell. 9:357-65.

Dorrell C, Tarlow B, Wang Y, Canaday PS, Haft A, Schug J, Streeter PR, Finegold MJ, Shenje LT, Kaestner KH, Grompe M. (2014). The organoid-initiating cells in mouse pancreas and liver are phenotypically and functionally similar. Stem Cell Res. 13:275-83.

Du YC, Chou CK, Klimstra DS, Varmus H. (2011). Receptor for hyaluronan-mediated motility isoform B promotes liver metastasis in a mouse model of multistep tumorigenesis and a tail vein assay for metastasis. Proc. Natl. Acad. Sci. USA. 108:16753-16758.

Emmink BL, Van Houdt WJ, Vries RG, Hoogwater FJ, Govaert KM, Verheem A, Nijkamp MW, Steller EJ, Jimenez CR, Clevers H, Borel Rinkes IH, Kranenburg O. (2011). Differentiated human colorectal cancer cells protect tumor-initiating cells from irinotecan. Gastroenterology. 141:269-78.

Eramo A, Lotti F, Sette G, Pilozzi E, Biffoni M, Di Virgilio A, Conticello C, Ruco L, Peschle C, De Maria R. (2008). Identification and expansion of the tumorigenic lung cancer stem cell population. Cell Death Differ. 15:504-14.

Falchetti A. (2017). Genetics of multiple endocrine neoplasia type 1 syndrome: what's new and what's old. F1000Res. 6, F1000 Faculty Rev-73.

Franko J, Feng W, Yip L, Genovese E, Moser AJ. (2010). Non-functional neuroendocrine carcinoma of the pancreas: incidence, tumor biology, and outcomes in 2,158 patients. J. Gastrointest. Surg. 14:541-548.

Fujii E, Suzuki M, Matsubara K, Watanabe M, Chen YJ, Adachi K, Ohnishi Y, Tanigawa M, Tsuchiya M, Tamaoki N. (2008). Establishment and characterization of *in vivo* human tumor models in the NOD/SCID/gamma(c)(null) mouse. Pathol Int. 58:559-67.

Fumagalli A, Oost KC, Kester L, Morgner J, Bornes L, Bruens L, Spaargaren L, Azkanaz M, Schelfhorst T, Beerling E, Heinz MC, Postrach D, Seinstra D, Sieuwerts AM, Martens JWM, van der Elst S, van Baalen M, Bhowmick D, Vrisekoop N, Ellenbroek SIJ, Suijkerbuijk SJE, Snippert HJ, van Rheenen J. (2020)**.** Plasticity of Lgr5-Negative Cancer Cells Drives Metastasis in Colorectal Cancer. Cell Stem Cell. 26:569-578.e7.

Gierl MS, Karoulias N, Wende H, Strehle M, Birchmeier C. (2006). The zinc-finger factor Insm1 (IA-1) is essential for the development of pancreatic beta cells and intestinal endocrine cells. Genes Dev. 20:2465-78.

Goto Y, De Silva MG, Toscani A, Prabhakar BS, Notkins AL, Lan MS. (1992). A novel human insulinoma-associated cDNA, IA-1, encodes a protein with "zinc-finger" DNA-binding motifs. J Biol Chem. 267:15252-7.

Grant SG, Seidman I, Hanahan D, Bautch VL. (1991) Early invasiveness characterizes metastatic carcinoid tumors in transgenic mice. Cancer Res. 51:4917-4923.

Greaves M, Maley CC. (2012). Clonal evolution in cancer. Nature. 481:306-13.

Gupta PB, Fillmore CM, Jiang G, Shapira SD, Tao K, Kuperwasser C, Lander ES. (2011). Stochastic state transitions give rise to phenotypic equilibrium in populations of cancer cells. Cell. 146:633-44.

Hager JC, Fligiel S, Stanley W, Richardson AM, Heppner GH. (1981). Characterization of a variant-producing tumor cell line from a heterogeneous strain BALB/cfC3H mouse mammary tumor. Cancer Res. 41:1293-1300.

Hanahan D. (1985). Heritable formation of pancreatic beta-cell tumours in transgenic mice expressing recombinant insulin/simian virus 40 oncogenes. Nature. 315:115–122.

Hanahan D, Weinberg RA. (2011). Hallmarks of cancer: the next generation. Cell. 144:646-64.

Hermann PC, Huber SL, Herrler T, Aicher A, Ellwart JW, Guba M, Bruns CJ, Heeschen C. (2007). Distinct populations of cancer stem cells determine tumor growth and metastatic activity in human pancreatic cancer. Cell Stem Cell. 1:313-23.

Jacques TS, Swales A, Brzozowski MJ, Henriquez NV, Linehan JM, Mirzadeh Z, O' Malley C, Naumann H, Alvarez-Buylla A, Brandner S. (2010). Combinations of genetic mutations in the adult neural stem cell compartment determine brain tumour phenotypes. EMBO J. 29:222-35.

Jung YS, Park JI. (2020)**.** Wnt signaling in cancer: therapeutic targeting of Wnt signaling beyond beta-catenin and the destruction complex. Exp Mol Med. 52:183-191.

Junttila MR, de Sauvage FJ. (2013). Influence of tumour micro-environment heterogeneity on therapeutic response. Nature. 501:346-54.

Kouros-Mehr H, Bechis SK, Slorach EM, Littlepage LE, Egeblad M, Ewald AJ, Pai SY, Ho IC, Werb Z. (2008). GATA-3 links tumor differentiation and dissemination in a luminal breast cancer model. Cancer Cell. 13:141-52.

Kremer L, Márquez G. (2004). Generation of monoclonal antibodies against chemokine receptors. Methods Mol Biol. 239:243-60.

Kreso A, Dick JE. (2014). Evolution of the cancer stem cell model. Cell Stem Cell. 14:275-91.

Kuo EJ, Salem RR. (2013). Population-level analysis of pancreatic neuroendocrine tumors 2 cm or less in size. Ann. Surg. Oncol. 20:2815–2821.

Lapidot T, Sirard C, Vormoor J, Murdoch B, Hoang T, Caceres-Cortes J, Minden M, Paterson B, Caligiuri MA, Dick JE. (1994). A cell initiating human acute myeloid leukaemia after transplantation into SCID mice. Nature. 367:645-8.

Lawson DA, Bhakta NR, Kessenbrock K, Prummel KD, Yu Y, Takai K, Zhou A, Eyob H, Balakrishnan S, Wang CY, Yaswen P, Goga A, Werb Z. (2015). Single-cell analysis reveals a stem-cell program in human metastatic breast cancer cells. Nature. 2015 526:131-5.

Li C, Heidt DG, Dalerba P, Burant CF, Zhang L, Adsay V, Wicha M, Clarke MF, Simeone DM. (2007). Identification of pancreatic cancer stem cells. Cancer Res. 67:1030-7.

Liu JC, Voisin V, Wang S, Wang DY, Jones RA, Datti A, Uehling D, Al-awar R, Egan SE, Bader GD, Tsao M, Mak TW, Zacksenhaus E. (2014). Combined deletion of Pten and p53 in mammary epithelium accelerates triple-negative breast cancer with dependency on eEF2K. EMBO Mol Med. 6:1542-60.

Lopez T, Hanahan D. (2002). Elevated levels of IGF-1 receptor convey invasive and metastatic capability in a mouse model of pancreatic islet tumorigenesis. Cancer Cell. 1:339–353.

Ma Z, Guo D, Wang Q, Liu P, Xiao Y, Wu P, Wang Y, Chen B, Liu Z, Liu Q. (2019). Lgr5-mediated p53 Repression through PDCD5 leads to doxorubicin resistance in Hepatocellular Carcinoma. Theranostics. 9:2967-2983.

Mani SA, Guo W, Liao MJ, Eaton EN, Ayyanan A, Zhou AY, Brooks M, Reinhard F, Zhang CC, Shipitsin M, Campbell LL, Polyak K, Brisken C, Yang J, Weinberg RA. (2008). The epithelial-mesenchymal transition generates cells with properties of stem cells. Cell. 133:704-15.

Meacham CE, Morrison SJ. (2013). Tumour heterogeneity and cancer cell plasticity. Nature. 501:328-37.

Nguyen LV, Vanner R, Dirks P, Eaves CJ. (2012). Cancer stem cells: an evolving concept. Nat Rev Cancer. 12:133-43.

O'Brien CA, Pollett A, Gallinger S, Dick JE. (2007). A human colon cancer cell capable of initiating tumour growth in immunodeficient mice. Nature. 445:106-10.

Olson P, Chu GC, Perry SR, Nolan-Stevaux O, Hanahan D. (2011). Imaging guided trials of the angiogenesis inhibitor sunitinib in mouse models predict efficacy in pancreatic neuroendocrine but not ductal carcinoma. Proc. Natl. Acad. Sci. USA. 108:E1275-E1284.

Osipovich AB, Long Q, Manduchi E, Gangula R, Hipkens SB, Schneider J, Okubo T, Stoeckert CJ Jr, Takada S, Magnuson MA. (2014). Insm1 promotes endocrine cell differentiation by modulating the expression of a network of genes that includes Neurog3 and Ripply3. Development. 141:2939-49.

Pak JN, Jung JH, Park JE, Hwang J, Lee HJ, Shim BS, Kim SH. (2020). p53 dependent LGR5 inhibition and caspase 3 activation are critically involved in apoptotic

effect of compound K and its combination therapy potential in HCT116 cells. Phytother Res. 34:2745-2755.

Patrawala L, Calhoun T, Schneider-Broussard R, Li H, Bhatia B, Tang S, Reilly JG, Chandra D, Zhou J, Claypool K, Coghlan L, Tang DG. (2006). Highly purified CD44+ prostate cancer cells from xenograft human tumors are enriched in tumorigenic and metastatic progenitor cells. Oncogene. 25:1696-708.

Pierce GB Jr, Dixon FJ Jr, Verney EL. (1960). Teratocarcinogenic and tissue-forming potentials of the cell types comprising neoplastic embryoid bodies Lab. Invest. 9:583-602.

Pierce GB, Cox WF. (1978). Neoplasms as caricatures of tissue renewal. Cell differentiation and neoplasia, Rave Press, New York. 1996-2004.

Pierce GB, Speers WC. (1988). Tumors as caricatures of the process of tissue renewal: prospects for therapy by directing differentiation. Cancer Res. 48:1996-2004.

Pollard SM, Yoshikawa K, Clarke ID, Danovi D, Stricker S, Russell R, Bayani J, Head R, Lee M, Bernstein M, Squire JA, Smith A, Dirks P. (2009). Glioma stem cell lines expanded in adherent culture have tumor-specific phenotypes and are suitable for chemical and genetic screens. Cell Stem Cell. 4:568-80.

Prince ME, Sivanandan R, Kaczorowski A, Wolf GT, Kaplan MJ, Dalerba P, Weissman IL, Clarke MF, Ailles LE. (2007). Identification of a subpopulation of cells with cancer stem cell properties in head and neck squamous cell carcinoma. Proc Natl Acad Sci U S A. 104:973-8.

Pyonteck SM, Gadea BB, Wang HW, Gocheva V, Hunter KE, Tang LH, Joyce JA. (2012). Deficiency of the macrophage growth factor CSF-1 disrupts pancreatic neuroendocrine tumor development. Oncogene. 31:1459-67.

Quintana E, Shackleton M, Foster HR, Fullen DR, Sabel MS, Johnson TM, Morrison SJ. (2010). Phenotypic heterogeneity among tumorigenic melanoma cells from patients that is reversible and not hierarchically organized. Cancer Cell. 18:510-23.

Raymond E, Dahan L, Raoul JL, Bang YJ, Borbath I, Lombard-Bohas C, Valle J, Metrakos P, Smith D, Vinik A, Chen JS, Hörsch D, Hammel P, Wiedenmann B, Van Cutsem E, Patyna S, Lu DR, Blanckmeister C, Chao R, Ruszniewski P. (2011). Sunitinib malate for the treatment of pancreatic neuroendocrine tumors. N Engl J Med. 364:501-13.

Reya T, Clevers H. (2005). Wnt signalling in stem cells and cancer. Nature. 434:843-50.

Ricci-Vitiani L, Lombardi DG, Pilozzi E, Biffoni M, Todaro M, Peschle C, De Maria R. (2007). Identification and expansion of human colon-cancer-initiating cells. Nature. 445:111-5.

Roesch A, Fukunaga-Kalabis M, Schmidt EC, Zabierowski SE, Brafford PA, Vultur A, Basu D, Gimotty P, Vogt T, Herlyn M. (2010). A temporarily distinct subpopulation of slow-cycling melanoma cells is required for continuous tumor growth. Cell. 141:583-94.

Sato Y, Mukai K, Watanabe S, Goto M, Shimosato Y. (1986). The AMeX method. A simplified technique of tissue processing and paraffin embedding with improved preservation of antigens for immunostaining. Am J Pathol. 125:431-5.

Scheel C, Eaton EN, Li SH, Chaffer CL, Reinhardt F, Kah KJ, Bell G, Guo W, Rubin J, Richardson AL, Weinberg RA. (2011). Paracrine and autocrine signals induce and maintain mesenchymal and stem cell states in the breast. Cell. 145:926-40.

Sennino B, Ishiguro-Oonuma T, Schriver BJ, Christensen JG, McDonald DM. (2013).Inhibition of c-Met reduces lymphatic metastasis in RIP-Tag2 transgenic mice. Cancer Res. 73:3692–3703.

Sharma SV, Lee DY, Li B, Quinlan MP, Takahashi F, Maheswaran S, McDermott U, Azizian N, Zou L, Fischbach MA, Wong KK, Brandstetter K, Wittner B, Ramaswamy S, Classon M, Settleman J. (2010). A chromatin-mediated reversible drug-tolerant state in cancer cell subpopulations. Cell. 141:69-80.

Singh SK, Hawkins C, Clarke ID, Squire JA, Bayani J, Hide T, Henkelman RM, Cusimano MD, Dirks PB. (2004). Identification of human brain tumour initiating cells. Nature. 432:396-401.

Suzuki M, Katsuyama K, Adachi K, Ogawa Y, Yorozu K, Fujii E, Misawa Y, Sugimoto T. (2002). Combination of fixation using PLP fixative and embedding in paraffin by the AMeX method is useful for histochemical studies in assessment of immunotoxicity. J Toxicol Sci. 27:165-72.

Takahashi K, Yamanaka S. (2006). Induction of pluripotent stem cells from mouse embryonic and adult fibroblast cultures by defined factors. Cell. 126:663-676.

Takahashi H, Ishii H, Nishida N, Takemasa I, Mizushima T, Ikeda M, Yokobori T, Mimori K, Yamamoto H, Sekimoto M, Doki Y, Mori M. (2011). Significance of Lgr5(+ve) cancer stem cells in the colon and rectum. Ann Surg Oncol. 18:1166-74.

Takeda K, Kinoshita I, Shimizu Y, Matsuno Y, Shichinohe T, Dosaka-Akita H. (2011). Expression of LGR5, an intestinal stem cell marker, during each stage of colorectal tumorigenesis. Anticancer Res. 31:263-70.

Takeda N, Jain R, LeBoeuf MR, Wang Q, Lu MM, Epstein JA. (2011). Interconversion between intestinal stem cell populations in distinct niches. Science. 334:1420-4.

Tian H, Biehs B, Warming S, Leong KG, Rangell L, Klein OD, de Sauvage FJ. (2011). A reserve stem cell population in small intestine renders Lgr5-positive cells dispensable. Nature. 478:255-9.

Todaro M, Alea MP, Di Stefano AB, Cammareri P, Vermeulen L, Iovino F, Tripodo C, Russo A, Gulotta G, Medema JP, Stassi G. (2007). Colon cancer stem cells dictate tumor growth and resist cell death by production of interleukin-4. Cell Stem Cell. 1:389-402.

Vermeulen L, Todaro M, de Sousa Mello F, Sprick MR, Kemper K, Perez Alea M, Richel DJ, Stassi G, Medema JP. (2008). Single-cell cloning of colon cancer stem cells reveals a multi-lineage differentiation capacity. Proc Natl Acad Sci U S A. 105:13427-32.

Vermeulen L, De Sousa E Melo F, van der Heijden M, Cameron K, de Jong JH, Borovski T, Tuynman JB, Todaro M, Merz C, Rodermond H, Sprick MR, Kemper K, Richel DJ, Stassi G, Medema JP. (2010). Wnt activity defines colon cancer stem cells and is regulated by the microenvironment. Nat Cell Biol. 12:468-76.

Wang Y, Jing Y, Ding L, Zhang X, Song Y, Chen S, Zhao X, Huang X, Pu Y, Wang Z, Ni Y, Hu Q. (2019). Epiregulin reprograms cancer-associated fibroblasts and facilitates oral squamous cell carcinoma invasion via JAK2-STAT3 pathway. J Exp Clin Cancer Res. 38:274.

Winslow MM, Dayton TL, Verhaak RG, Kim-Kiselak C, Snyder EL, Feldser DM, Hubbard DD, DuPage MJ, Whittaker CA, Hoersch S, Yoon S, Crowley D, Bronson RT, Chiang DY, Meyerson M, Jacks T. (2011). Suppression of lung adenocarcinoma progression by Nkx2-1. Nature. 473:101-4.

Wiwatpanit T, Lorenzen SM, Cantú JA, Foo CZ, Hogan AK, Márquez F, Clancy JC, Schipma MJ, Cheatham MA, Duggan A, García-Añoveros J. (2018). Trans-differentiation of outer hair cells into inner hair cells in the absence of INSM1. Nature. 563:691-695.

Wu C, Wei Q, Utomo V, Nadesan P, Whetstone H, Kandel R, Wunder JS, Alman BA. (2007). Side population cells isolated from mesenchymal neoplasms have tumor initiating potential. Cancer Res. 67:8216-22.

Yao JC, Shah MH, Ito T, Bohas CL, Wolin EM, Van Cutsem E, Hobday TJ, Okusaka T, Capdevila J, de Vries EG, Tomassetti P, Pavel ME, Hoosen S, Haas T, Lincy J, Lebwohl D, Öberg K. (2011). Everolimus for advanced pancreatic neuroendocrine tumors. N Engl J Med. 364:514-23.

Zhang T, Wang H, Saunee NA, Breslin MB, Lan MS. (2010). Insulinoma-associated antigen-1 zinc-finger transcription factor promotes pancreatic duct cell trans-differentiation. Endocrinology. 151:2030-2039.

Zhang T, Saunee NA, Breslin MB, Song K, Lan MS. (2012). Functional role of an islet transcription factor, INSM1/IA-1, on pancreatic acinar cell trans-differentiation. J Cell Physiol. 227:2470-9.

Zhong Z, Virshup DM. (2020)**.** Wnt Signaling and Drug Resistance in Cancer. Mol Pharmacol. 97:72-89.